

# 1 Truncated denitrifiers dominate the denitrification 2 pathway in tundra soil metagenomes

3 Igor S. Pessi<sup>1,2</sup>, Sirja Viitamäki<sup>1</sup>, Anna-Maria Virkkala<sup>3,4</sup>, Eeva Eronen-Rasimus<sup>1,5</sup>,  
4 Tom O. Delmont<sup>6</sup>, Maija E. Marushchak<sup>7,8</sup>, Miska Luoto<sup>3</sup>, and Jenni Hultman<sup>1,2,9,\*</sup>

5 <sup>1</sup>Department of Microbiology, University of Helsinki, Helsinki, Finland

6 <sup>2</sup>Helsinki Institute of Sustainability Science (HELSUS), Helsinki, Finland

7 <sup>3</sup>Department of Geosciences and Geography, University of Helsinki, Helsinki, Finland

8 <sup>4</sup>Woodwell Climate Research Center, Falmouth, MA, USA

9 <sup>5</sup>Marine Research Centre, Finnish Environment Institute (SYKE), Helsinki, Finland

10 <sup>6</sup>Department of Bioinformatics, Genoscope, Paris, France

11 <sup>7</sup>Department of Biological and Environmental Science, University of Jyväskylä, Jyväskylä, Finland

12 <sup>8</sup>Department of Environmental and Biological Sciences, University of Eastern Finland, Kuopio, Finland

13 <sup>9</sup>Natural Resources Institute Finland (Luke), Helsinki, Finland

14 \*Corresponding author: [jenni.hultman@helsinki.fi](mailto:jenni.hultman@helsinki.fi)

## 15 Abstract

16 In contrast to earlier assumptions, there is now mounting evidence for the role of tundra soils  
17 as important sources of the greenhouse gas nitrous oxide (N<sub>2</sub>O). However, the microorganisms  
18 involved in the cycling of N<sub>2</sub>O in this system remain largely uncharacterized. Since tundra soils  
19 are variable sources and sinks of N<sub>2</sub>O we aimed to investigate the links between microbial  
20 community structure and N<sub>2</sub>O cycling in this system. We analysed 1.4 Tb of metagenomic data  
21 and manually binned and curated 796 metagenome-assembled genomes (MAGs) from soils in  
22 northern Finland covering a range of ecosystems from dry upland soils to water-logged fens. We  
23 then searched for MAGs harbouring genes involved in denitrification, an important biotic  
24 process driving N<sub>2</sub>O emissions. Communities of potential denitrifiers were dominated by  
25 microorganisms with truncated denitrification pathways (i.e. lacking one or more denitrification  
26 genes) and differed across soil ecosystems. Upland soils had a strong N<sub>2</sub>O sink potential and  
27 were dominated by members of the Alphaproteobacteria such as *Bradyrhizobium* and  
28 *Reyranella*. Fens, which had in general net-zero N<sub>2</sub>O fluxes, had a high abundance of poorly  
29 characterized taxa affiliated with the Chloroflexota lineage Ellin6529 and the Acidobacteriota  
30 subdivision Gp23. By coupling an in-depth characterization of microbial communities with *in*  
31 *situ* measurements of N<sub>2</sub>O fluxes, our results suggest that the observed spatial patterns of N<sub>2</sub>O  
32 cycling are driven by the composition of denitrifier communities.

## 33 Background

34 Nitrous oxide (N<sub>2</sub>O) is a greenhouse gas (GHG) that has approximately 300 times the global  
35 warming potential of carbon dioxide on a 100-year scale [1]. Atmospheric N<sub>2</sub>O concentrations  
36 have increased by nearly 20% since pre-industrial times, with soils – both natural and  
37 anthropogenic – accounting for up to 70% of the global emissions [2]. Despite being nitrogen (N)  
38 limited and enduring low temperatures throughout most of the year, tundra soils are  
39 increasingly recognized as important sources of N<sub>2</sub>O [3–7]. The relative contribution of tundra  
40 soils to global GHG emissions is predicted to increase in the future [8, 9], as the warming rate  
41 at high latitude environments is more than twice as high than in other regions [10].

42 Microbial denitrification is an important biotic source of N<sub>2</sub>O [11]. Denitrification is a series of  
43 enzymatic steps in which nitrate (NO<sub>3</sub><sup>-</sup>) is sequentially reduced to nitrite (NO<sub>2</sub><sup>-</sup>), nitric oxide  
44 (NO), N<sub>2</sub>O, and dinitrogen (N<sub>2</sub>) via the activity of the Nar, Nir, Nor, and Nos enzymes,  
45 respectively. The denitrification trait is common across a wide range of archaea, bacteria, and  
46 some fungi, most of which are facultative anaerobes that switch to N oxides as electron acceptor  
47 when oxygen becomes limiting [12]. Denitrification is a modular community process performed  
48 in synergy by different microbial taxa that execute only a subset of the complete denitrification  
49 pathway [12, 13]. With the growing number of microbial genomes sequenced in recent years, it  
50 has become evident that only a fraction of the microorganisms involved in the denitrification  
51 pathway encode the enzymatic machinery needed for complete denitrification [14, 15]. For  
52 instance, a study that investigated 652 genomes of cultured denitrifiers showed that  
53 approximately 31% encode the full set of enzymes needed for complete denitrification [14].

54 Modelling N<sub>2</sub>O emissions based on microbial community structure is challenging. N<sub>2</sub>O fluxes  
55 are characterized by a high temporal and spatial heterogeneity driven by several environmental  
56 constraints related to soil pH, N, moisture, and oxygen content [11]. In addition, our knowledge  
57 of the regulation of the denitrification process is largely based on the activity of model organisms  
58 such as the complete denitrifier *Paracoccus denitrificans* [16]. It has been suggested that  
59 incomplete denitrifiers that contain Nir and Nor but lack Nos contribute substantially to soil  
60 N<sub>2</sub>O emissions [17], while non-denitrifying N<sub>2</sub>O reducers, i.e. microorganisms that contain Nos  
61 but lack Nir, can represent an important N<sub>2</sub>O sink [18–20]. Furthermore, the partitioning of  
62 metabolic pathways across different populations with truncated pathways – also known as  
63 metabolic handoffs [21] – has been linked to higher efficiencies in substrate consumption  
64 compared to complete pathways [15, 22]. However, it remains largely unclear how populations  
65 of truncated denitrifiers with different sets of denitrification genes interact with each other and  
66 the environment impacting N<sub>2</sub>O emissions *in situ*.

67 Compared to high N<sub>2</sub>O-emitting systems such as agricultural and tropical soils, our knowledge  
68 of denitrifier communities in tundra soils is limited. As denitrification leads to the loss of N to  
69 the atmosphere, it enhances the N-limited status of tundra systems thus impacting both  
70 microbial and plant communities [23, 24]. Investigations of denitrifier diversity in the tundra  
71 have been largely limited to gene-centric surveys using microarrays, amplicon sequencing,  
72 qPCR, and read-based metagenomics, which provide limited information on the taxonomic  
73 identity and genomic composition of community members. These studies have shown that  
74 denitrifier communities in the tundra are dominated by members of the phyla Proteobacteria,  
75 Actinobacteria, and Bacteroidetes, and that the potential for complete denitrification is usually  
76 present at the community level [25–29]. However, it is not known whether the complete  
77 denitrification potential occurs within discrete microbial populations or is widespread  
78 throughout populations of truncated denitrifiers lacking one or more denitrification genes. In  
79 addition, tundra soils encompass many different ecosystems, some of which are notorious N<sub>2</sub>O  
80 sources (e.g. bare peat surfaces [3]). N<sub>2</sub>O consumption is usually favoured in wetlands, where  
81 low NO<sub>3</sub><sup>-</sup> availability due to anoxia promotes the reduction of N<sub>2</sub>O to N<sub>2</sub> [30]. In upland soils,  
82 N<sub>2</sub>O fluxes vary in both time and space. Strong N<sub>2</sub>O sinks have been observed specially in  
83 sparsely vegetated upland soils [7], but the microbial processes underlying N<sub>2</sub>O consumption in  
84 these systems are largely unknown [31]. Altogether, these large differences in N<sub>2</sub>O fluxes across  
85 tundra ecosystems indicate differences in the structure of microbial communities, but a  
86 comprehensive understanding of the microorganisms driving N<sub>2</sub>O cycles in tundra soils is  
87 lacking.

88 The paucity of in-depth knowledge on denitrifying communities in the tundra impairs our  
89 ability to model current and future N<sub>2</sub>O fluxes from this biome. A better understanding of the  
90 ecological, metabolic, and functional traits of denitrifiers is thus critical for improving current  
91 models and mitigating N<sub>2</sub>O emissions [32]. This invariably relies on the characterization of the  
92 so-called uncultured majority, i.e. microorganisms that have not been cultured to date but which  
93 comprise a high proportion of the microbial diversity in complex ecosystems [33, 34]. Genome-  
94 resolved metagenomics is a powerful tool to access the genomes of uncultured microorganisms  
95 and has provided important insights into carbon cycling processes in tundra soils [35–37].  
96 However, this approach has not yet been applied to investigate the mechanisms driving N<sub>2</sub>O  
97 cycling in the tundra. Here, we used genome-resolved metagenomics to investigate the diversity  
98 and metabolic capabilities of potential denitrifiers across different tundra soil ecosystems  
99 characterised by a high variability in net N<sub>2</sub>O fluxes. Our aim was to elucidate the  
100 denitrification potential of microbial populations and explore the relationship between  
101 microbial community structure and patterns of N<sub>2</sub>O fluxes in these ecosystems. For this, we

102 analysed 1.4 Tb of metagenomic data from 69 soil samples from an area of mountain tundra  
103 biome in Kilpisjärvi, northern Finland, and obtained 796 manually curated metagenome-  
104 assembled genomes (MAGs).

## 105 **Methods**

### 106 **Study area and sampling for metagenomic analysis**

107 The Saana Nature Reserve (69.04°N, 20.79°E) is located in Kilpisjärvi, northern Finland  
108 **(Suppl. Fig. S1a)**. The area is part of the mountain tundra biome and is characterized by a  
109 mean annual temperature of  $-1.9^{\circ}\text{C}$  and annual precipitation of 487 mm [38]. Our study sites  
110 are distributed across Mount Saana and Mount Korkea-Jehkas and the valley in between  
111 **(Suppl. Fig. S1b)**, and include barren soils, heathlands (dominated by evergreen and deciduous  
112 shrubs), meadows (dominated by graminoids and forbs), and fens **(Suppl. Fig. S1c)**. In previous  
113 studies, we have established in the area a systematic fine-scale sampling of microclimate, soil  
114 conditions, and vegetation in topographically distinct environments [39–41]. Local variation in  
115 topography and soil properties creates a mosaic of habitats characterized by contrasting  
116 ecological conditions. This makes the study setting ideal to investigate species-environment  
117 relationships and ecosystem functioning in the tundra [41–43].

118 Sampling for metagenomic analysis was performed across 43 sites (barren soils,  $n = 2$ ;  
119 heathlands,  $n = 18$ ; meadows,  $n = 7$ ; fens,  $n = 16$ ) in July 2017 and July 2018, during the growing  
120 season in the northern hemisphere. Samples were obtained with a soil corer sterilized with 70%  
121 ethanol and, when possible, cores were split into organic and mineral samples using a sterilized  
122 spatula. In total, 41 organic and 28 mineral samples were obtained for metagenomic analysis  
123 **(Suppl. Table S1)**. Samples were transferred to a whirl-pack bag and immediately frozen in  
124 dry ice. Samples were transported frozen to the laboratory at the University of Helsinki and  
125 kept at  $-80^{\circ}\text{C}$  until analyses.

### 126 **Soil physicochemical characterization and *in situ* measurement of GHG fluxes**

127 Soil physicochemical characterization was done using an extended set of 228 sites distributed  
128 across the study area. Soil pH, moisture, and soil organic matter (SOM) content were measured  
129 according to Finnish (SFS) and international (ISO) standards (SFS 300, ISO 10390, and SFS  
130 3008). Carbon (C) and N content were measured using a Vario Micro Cube machine (Elementar,  
131 Langenselbold, Germany). *In situ* ecosystem-level  $\text{N}_2\text{O}$  and methane ( $\text{CH}_4$ ) fluxes were  
132 measured from 101 sites using a static, non-steady state, non-flow-through system composed of  
133 a darkened acrylic chamber (20 cm diameter, 25 cm height) [4, 44]. Measurements were

134 conducted between 2<sup>nd</sup> July and 2<sup>nd</sup> August 2018, between 10 am and 5 pm. Simultaneous  
135 measurement of GHG fluxes and sampling for metagenomic sequencing was not possible due to  
136 limited resources and logistic constraints. At each site, five 25 mL gas samples were taken  
137 during a 50-minute chamber closure and transferred to evacuated Exetainer vials (Labco,  
138 Lampeter, UK). Gas samples were analysed using an Agilent 7890B gas chromatograph (Agilent  
139 Technologies, Santa Clara, CA, USA) equipped with an autosampler (Gilson, Middleton, WI,  
140 USA) and a flame ionization detector for CH<sub>4</sub> and an electron capture detector for N<sub>2</sub>O. Gas  
141 concentrations were calculated from the gas chromatograph peak areas based on standard  
142 curves with a CH<sub>4</sub> concentration of 0–100 ppm and a N<sub>2</sub>O concentration of 0–5000 ppb.  
143 Differences in physicochemical composition and rates of GHG fluxes across soil ecosystems were  
144 assessed using one-way analysis of variance (ANOVA) followed by Tukey’s HSD test with the  
145 *lm* and *TukeyHSD* functions in R v3.6.3 [45].

## 146 **Metagenome sequencing and processing of raw data**

147 Total DNA and RNA were co-extracted as previously described [41]. Briefly, extraction was  
148 performed on 0.5 g of soil using a hexadecyltrimethyl ammonium bromide (CTAB), phenol-  
149 chloroform, and bead-beating protocol. DNA was purified using the AllPrep DNA Mini Kit  
150 (QIAGEN, Hilden, Germany) and quantified using the Qubit dsDNA BR Assay Kit  
151 (ThermoFisher Scientific, Waltham, MA, USA). Library preparation for Illumina metagenome  
152 sequencing was performed using the Nextera XT DNA Library Preparation Kit (Illumina, San  
153 Diego, CA, USA). Metagenomes were obtained for 69 samples across two paired-end NextSeq  
154 (132–170 bp) and one NovaSeq (2 x 151 bp) runs (**Suppl. Table S1**). Two samples were  
155 additionally sequenced with Nanopore MinION. For this, libraries were prepared using the  
156 SQK-LSK109 Ligation Sequencing Kit with the long fragment buffer (Oxford Nanopore  
157 Technologies, Oxford, UK) and the NEBNext Companion Module for Oxford Nanopore  
158 Technologies Ligation Sequencing Kit (New England Biolabs). Each sample was sequenced for  
159 48 hours on one R9.4 flow cell.

160 The quality of the raw Illumina data was verified with fastQC v0.11.9 [46] and multiQC v1.8  
161 [47]. Cutadapt v1.16 [48] was then used to trim sequencing adapters and low-quality base calls  
162 ( $q < 20$ ) and to filter out short reads ( $< 50$  bp). Nanopore data were basecalled with GPU guppy  
163 v4.0.11 using the high-accuracy model and applying a minimum quality score of 7. The quality  
164 of the basecalled Nanopore data was assessed with pycoQC v2.5.0.21 [49] and adapters were  
165 trimmed with Porechop v0.2.4 [50].

## 166 **Taxonomic profiling**

167 Taxonomic profiles of the microbial communities were obtained using a read-based approach,  
168 i.e. based on unassembled Illumina data. Due to differences in sequencing depth across the  
169 samples, the dataset was resampled to 2,000,000 reads per sample with seqtk v1.3 [51]. Reads  
170 matching the SSU rRNA gene were identified with METAXA v2.2 [52] and classified against  
171 the SILVA database release 138.1 [53] in mothur v1.44.3 [54] using the Wang's Naïve Bayesian  
172 Classifier [55] and a 80% confidence cut-off. Differences in community structure were assessed  
173 using non-metric multidimensional scaling (NMDS) and permutational ANOVA  
174 (PERMANOVA) with the package vegan v2.5.6 [56] in R v3.6.3 [45] (functions *metaMDS* and  
175 *adonis*, respectively).

## 176 **Metagenome assembling and binning**

177 Metagenome assembling of the Illumina data was performed as two co-assemblies. One co-  
178 assembly comprised the upland soils (barren, heathland, and meadow; n = 47) and the other the  
179 fen samples (n = 22). For each co-assembly, reads from the respective samples were pooled and  
180 assembled with MEGAHIT v1.1.1.2 [57]. Assembling of the Nanopore data was done for each  
181 sample individually with metaFlye v2.7.1 [58], and contigs were corrected based on Illumina  
182 data from the respective sample with bowtie v2.3.5 [59], SAMtools v1.9 [60], and pilon v1.23  
183 [61]. Quality assessment of the (co-)assemblies was obtained with metaQUAST v5.0.2 [62].

184 MAG binning was done separately for each Illumina and Nanopore (co-)assembly with anvi'o  
185 v6.2 [63] after discarding contigs shorter than 2500 bp. Gene calls were predicted with prodigal  
186 v2.6.3 [64]. Single-copy genes were identified with HMMER v.3.2.1 [65] and classified with  
187 DIAMOND v0.9.14 [66] against the Genome Taxonomy Database (GTDB) release 04-RS89 [67,  
188 68]. Illumina reads were mapped to the contigs with bowtie v2.3.5 [59] and SAM files were  
189 sorted and indexed using SAMtools v1.9 [60]. Due to their large sizes, Illumina co-assemblies  
190 were split into 100 smaller clusters based on differential coverage and tetranucleotide frequency  
191 with CONCOCT v1.0.0 [69]. Contigs were then manually sorted into bins based on the same  
192 composition and coverage metrics using the *anvi-interactive* interface in anvi'o v6.2 [63].  
193 Nanopore contigs were binned directly without pre-clustering. Bins that were  $\geq 50\%$  complete  
194 according to the presence of single-copy genes were further refined using the *anvi-refine*  
195 interface in anvi'o v6.2 [63]. In addition to taxonomic signal (based on single-copy genes  
196 classified against GTDB), either differential coverage or tetranucleotide frequency was used to  
197 identify and remove outlying contigs. The former was used for bins with a large variation in  
198 contig coverage across samples, and the latter for those with marked differences in GC content

199 across contigs. Bins  $\geq 50\%$  complete and  $\leq 10\%$  redundant – hereafter referred as MAGs – were  
200 kept for downstream analyses.

## 201 **Gene-centric analyses**

202 Functional profiles of the microbial communities were obtained using a gene-centric approach  
203 based on assembled data. For each (co-)assembly, gene calls were translated to amino acid  
204 sequences and searched against the KOfam hidden Markov model (HMM) database with  
205 KofamScan v1.3.0 [70]. Only matches with scores above the pre-computed family-specific  
206 thresholds were kept. Genes putatively identified as denitrification genes (*nirK*, *nirS*, *norB*, and  
207 *nosZ*) were submitted to further analyses. Amino acid sequences were aligned with MAFFT  
208 v7.429 [71] and alignments were visualized with Unipro UGENE v38.1 [72]. Sequences were  
209 then inspected for the presence of conserved residues at the following positions: *nirK*, Cu-  
210 binding and active sites [73]; *nirS*, c-heme and d<sub>1</sub>-heme binding sites [74]; *norB*, binding of the  
211 catalytic centres cyt b, b<sub>3</sub>, and Fe<sub>b</sub> [75]; *nosZ*: binding of the Cu<sub>Z</sub> and Cu<sub>A</sub> centres [75]. Sequences  
212 which did not contain the correct amino acid at these positions were removed. Finally, resulting  
213 amino acid sequences were aligned with MAFFT v7.429 [71] along with reference sequences  
214 from Graf et al. [14] and a maximum-likelihood tree was computed with FastTree v2.1.11 [76]  
215 using the LG+GAMMA model. Annotation of denitrification genes was also performed for  
216 previously published genomes retrieved from GenBank. These included a set of 1529 MAGs  
217 obtained from soils in Stordalen Mire, northern Sweden [37], and all (n = 69) genomes of  
218 Acidobacteriota strains and candidate taxa (accessed on 9 October 2020).

219 The abundance of functional genes was computed based on read coverage with CoverM v0.6.1  
220 [77]. For this, Illumina reads were mapped to the contigs with minimap v2.17 [78] and coverage  
221 was normalized to reads per kilobase million (RPKM). Differences in functional community  
222 structure were assessed using NMDS and PERMANOVA as described above for the taxonomic  
223 profiles. Differences in the abundance of individual genes across soil ecosystems were assessed  
224 using ANOVA followed by Tukey's HSD test with the *lm* and *TukeyHSD* functions in R v3.6.3  
225 [45]. Relationships between the abundance of denitrification genes and N<sub>2</sub>O flux rates were  
226 assessed using linear regression in R v3.6.3 [45].

## 227 **Phylogenomic analyses of MAGs and metabolic reconstruction**

228 Phylogenetic placement of MAGs was done based on 122 archaeal and 120 bacterial single-copy  
229 genes with GTDB-Tk v1.3.0 [79] and the GTDB release 05-RS95 [67, 68]. Acidobacteriota MAGs  
230 containing denitrification genes were submitted to further phylogenomic analyses alongside all  
231 genomes of Acidobacteriota strains and candidate taxa available on GenBank (n = 69; accessed

232 on 9 October 2020). For this, the amino acid sequence of 23 ribosomal proteins was retrieved for  
233 each genome with *anvi'o* v6.2 [63] and aligned with MUSCLE v3.8.1551 [80]. A maximum  
234 likelihood tree was then computed based on the concatenated alignments with FastTree v2.1.11  
235 using the LG+GAMMA model [76]. *Escherichia coli* ATCC 11775 was used to root the tree.

236 For metabolic reconstruction, MAGs were annotated against the Kofam HMM database [70]  
237 with HMMER v.3.2.1 [65] using the pre-computed score thresholds of each HMM profile. The  
238 *anvi-estimate-metabolism* program in *anvi'o* v6.2 [63] was then used to predict the metabolic  
239 capabilities of the MAGs. A metabolic pathway was considered present in MAGs containing at  
240 least 75% of the genes involved in the pathway. Carbohydrate-active enzymes (CAZymes) were  
241 annotated with dbCAN v.2.0 based on the dbCAN v7 HMM database [81]. Only hits with an e-  
242 value  $< 1 \times 10^{-14}$  and coverage  $> 0.35$  were considered.

## 243 **MAG dereplication and read recruitment analysis**

244 Prior to read recruitment analyses, Illumina and Nanopore MAGs were dereplicated based on  
245 a 99% average nucleotide identity (ANI) threshold with fastANI v1.3 [82] to remove redundancy  
246 (i.e. MAGs that were recovered multiple times across the different assemblies). Read  
247 recruitment analyses were then performed with CoverM v0.6.1 [77]. For this, Illumina  
248 reads were mapped to the set of non-redundant MAGs with minimap v2.17 [78] and relative  
249 abundances were calculated as a proportion of the reads mapping to each MAG.

## 250 **Results**

### 251 **Environmental characterization and *in situ* GHG fluxes**

252 Our sampling design in Kilpisjärvi included two soil depths across four ecosystems that are  
253 characteristic of the tundra biome (barren soils, heathlands, meadows, and fens) (**Suppl.**  
254 **Figure S1a–c**). Soil ecosystems differed in vegetation cover and physicochemical composition,  
255 with fens in particular being characterized by higher pH, moisture, and N content (one-way  
256 ANOVA,  $R^2 = 0.16$ – $0.64$ ,  $p < 0.001$ ) and, together with the meadows, lower C:N ratio (one-way  
257 ANOVA,  $R^2 = 0.49$ ,  $p < 0.001$ ) (**Suppl. Fig. S1d**). *In situ* measurements of GHG fluxes showed  
258 a high sink-source variability in net  $N_2O$  fluxes across the ecosystems (**Suppl. Fig. S1e**).  
259 Although the average  $N_2O$  flux across all sites was small (net consumption of  
260  $6 \mu g N_2O m^{-2} day^{-1}$ ), high  $N_2O$  emission at rates of up to  $660 \mu g N_2O m^{-2} day^{-1}$  was observed at  
261 the meadow sites. Likewise, strong  $N_2O$  consumption (up to  $-435 \mu g N_2O m^{-2} day^{-1}$ ) was  
262 observed particularly at the heathland and meadow sites. Net  $CH_4$  emissions were observed  
263 exclusively at the fen sites (**Suppl. Fig. S1e**).



## 264 **Differences in microbial community structure across soils ecosystems**

265 We obtained more than 9 billion Illumina (1.4 Tb) and 7 million Nanopore (21.5 Gb) reads from  
266 the 69 soil metagenomes (mean: 19.9 Gb, minimum: 0.7 Gb, maximum: 82.9 Gb) (**Suppl. Table**  
267 **S1**). Two Illumina co-assemblies and two individual Nanopore assemblies yielded more than 4  
268 million contigs longer than 2,500 bp, with a total assembly size of 21.1 Gb. The co-assemblies  
269 covered a significant fraction of the original metagenomic data, with an average read  
270 recruitment rate of 54.6% across samples (minimum: 22.9%, maximum: 75.8%).

271 Read-based analyses of unassembled SSU rRNA gene sequences showed that microbial  
272 community composition differed across the ecosystems, with fen soils harbouring contrasting  
273 microbial communities compared to the other ecosystems (PERMANOVA,  $R^2 = 0.35$ ,  $p < 0.001$ )  
274 (**Suppl. Fig. S2a**). No differences in community structure were observed between soil depths  
275 or the interaction between soil ecosystem and depth (PERMANOVA,  $p > 0.05$ ). Among  
276 previously described (i.e. not unclassified) taxa, microbial communities in barren, heathland,  
277 and meadow soils were dominated by aerobic and facultative anaerobic heterotrophs such as  
278 *Acidipila/Silvibacterium*, *Bryobacter*, *Granulicella*, *Acidothermus*, *Conexibacter*,  
279 *Mycobacterium*, *Mucilaginibacter*, *Bradyrhizobium*, and *Roseiarcus* (**Suppl. Fig. S2b**). On the  
280 other hand, fen soils were dominated by methanogenic archaea from the genera  
281 *Methanobacterium* and *Methanosaeta* and anaerobic bacteria such as *Thermoanaerobaculum*,  
282 *Desulfobacca*, and *Smithella*, but also the putative aerobic heterotroph *Candidatus* Koribacter.

283 Communities from different ecosystems also differed in their functional potential (**Suppl. Fig.**  
284 **S2c**). Denitrification genes (*nirK*, *nirS*, *norB*, and *nosZ*) were in general more abundant in the  
285 meadows and fens (one-way ANOVA,  $R^2 = 0.48$ – $0.76$ ,  $p < 0.001$ ) (**Suppl. Fig. S2d**). These were  
286 annotated using a three-step approach to avoid false positives consisting of distantly related  
287 homologues that are not involved in denitrification. Putative genes were first identified by  
288 searching predicted amino acid sequences against curated HMMs from the KOfam database  
289 [70]. Positive matches were then aligned and manually inspected for the presence of conserved  
290 residues at specific positions associated with the binding of co-factors and active sites [73–75].  
291 Sequences containing the correct amino acid at these core positions were further submitted to  
292 phylogenetic analyses along with sequences from a comprehensive database of archaeal and  
293 bacterial genomes [14]. In addition to denitrification genes, fen soils also had a higher  
294 abundance of genes involved in sulfate reduction (*dsrA* and *dsrB*) and methanogenesis (*mcrA*  
295 and *mcrB*) (one-way ANOVA,  $R^2 = 0.59$ – $0.90$ ,  $p < 0.001$ ). We did not observe a significant  
296 relationship between  $N_2O$  flux rates and neither the abundance of individual denitrification  
297 genes nor the ratio between *nosZ* and *nirK+nirS* abundances (linear regression,  $p > 0.05$ ).

298 However, the ratio between *nosZ* and *nirK+nirS* abundances was higher in the meadows (one-  
299 way ANOVA,  $R^2 = 0.29$ ,  $p < 0.001$ ) (**Suppl. Fig. S2d**), which indicates a higher potential for  
300  $N_2O$  consumption in this ecosystem.

### 301 **A manually curated genomic database from tundra soil metagenomes**

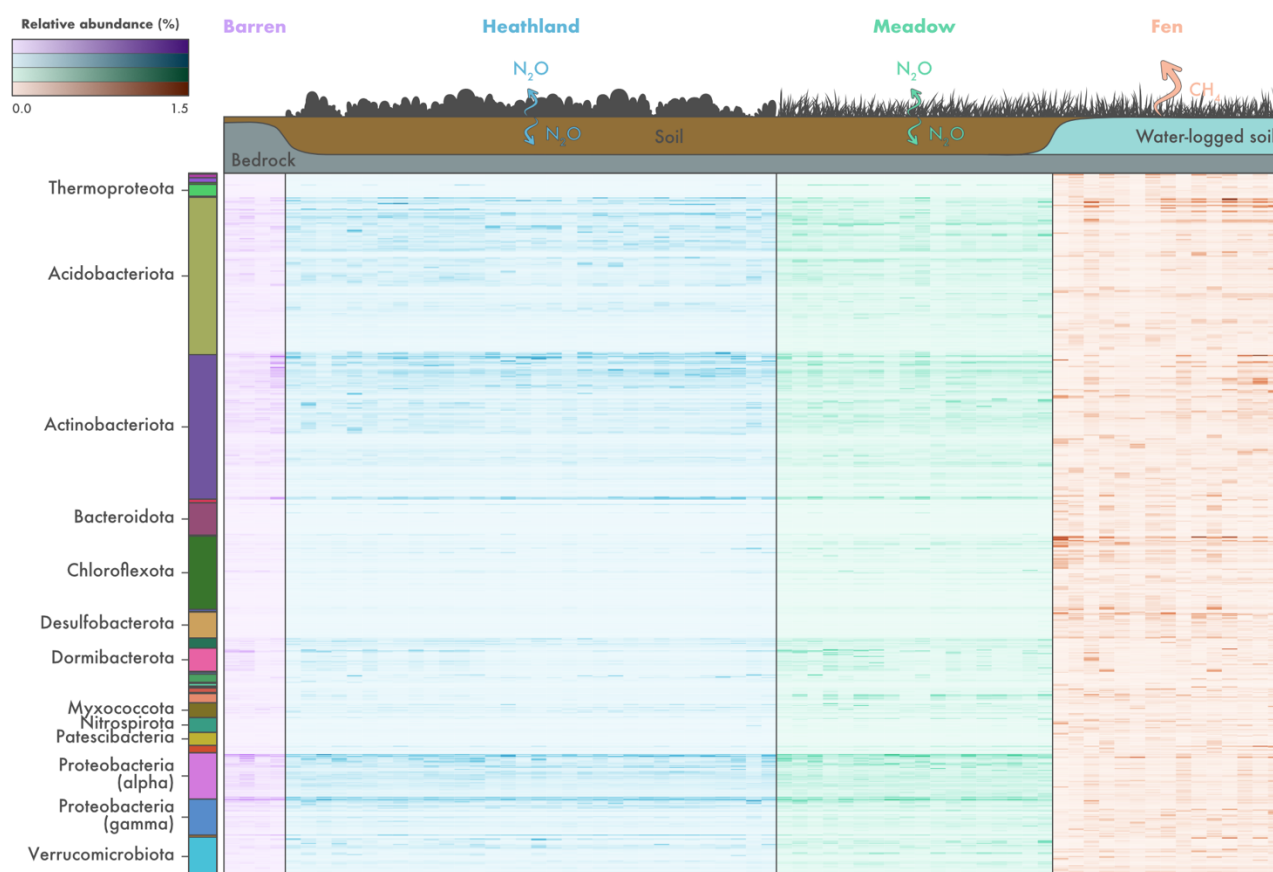
302 Using anvi'o [63], we obtained 8,043 genomic bins and manually curated these to a set of 796  
303 MAGs that were at least 50% complete and no more than 10% redundant (**Fig. 1, Suppl. Table**  
304 **S2**). According to estimates based on domain-specific single-copy genes, the obtained MAGs  
305 were on average 65.4% complete (minimum: 50.0%, maximum: 100.0%) and 2.7% redundant  
306 (minimum: 0.0%, maximum: 9.9%) (**Suppl. Table S2**). Phylogenomic analyses based on 122  
307 archaeal and 120 bacterial single-copy genes placed the MAGs across 35 bacterial and archaeal  
308 phyla according to the GTDB classification [67, 68] (**Fig. 1**). The most represented phyla were  
309 Acidobacteriota ( $n = 172$ ), Actinobacteriota ( $n = 163$ ), Proteobacteria (Alphaproteobacteria,  
310  $n = 54$ ; Gammaproteobacteria,  $n = 39$ ), Chloroflexota ( $n = 84$ ), and Verrucomicrobiota ( $n = 43$ ).  
311 Most MAGs ( $n = 703$ ) belonged to genera that do not comprise formally described species,  
312 including 303 MAGs that were placed outside genus-level lineages currently described in GTDB  
313 and thus likely represent novel genera (**Suppl. Table S2**).

314 To investigate their distribution across the different soil ecosystems, MAGs were dereplicated  
315 based on a 90% ANI threshold, yielding a set of 761 non-redundant MAGs (**Fig. 2**). On average,  
316 15.8% of the reads from each sample were recruited by the set of non-redundant MAGs  
317 (minimum: 7.6%, maximum: 30.5%). In agreement with the read-based assessment, we  
318 observed differences in MAG composition across the soil ecosystems, with only 50 MAGs shared  
319 between the heathland, meadow, and fen soils (**Suppl. Fig. S3a**). Fen soils harboured the  
320 highest number of MAGs, with an average of 155 MAGs per sample (**Suppl. Fig. S3b**).  
321 Although barren and fen soils had similar taxonomic richness according to the read-based  
322 estimates, only a small number of MAGs was detected in the barren soils (average of four MAGs  
323 per sample). This is likely a result of limited sampling and sequencing of this ecosystem, which  
324 consisted of four samples and a total of 7.9 Gb of metagenomic data (**Suppl. Table S1**). The  
325 number of MAGs in heathland and meadow soils was similar (average of 47 and 63 MAGs per  
326 sample, respectively) (**Suppl. Fig. S3b**). In general, barren, heathland, and meadow soils were  
327 dominated by the same set of MAGs (**Suppl. Fig. S3c**). These included members of the  
328 Acidobacteriota (*Sulfotelmato bacter* and unclassified genera in the class Acidobacteriae),  
329 Actinobacteriota (*Mycobacterium* and unclassified genera in the family Streptosporangiaceae),  
330 and Proteobacteria (Alphaproteobacteria: *Reyranella*, *Bradyrhizobium*, and unclassified  
331 Xanthobacteraceae; Gammaproteobacteria: unclassified Steroidobacteraceae). On the other

332 hand, fen soils were dominated by MAGs that were not assigned to formally described genera,  
333 including lineages of Acidobacteriota (family Koribacteraceae), Actinobacteriota (family  
334 Solirubrobacteraceae), Chloroflexota (class Ellin6529), Desulfobacterota (order  
335 Desulfobaccales), and Halobacterota.



336 **Fig. 1 | Genome-resolved metagenomics of tundra soils.** Phylogenomic placement and  
337 assembly statistics of 796 metagenome-assembled genomes (MAGs) recovered from soils in  
338 Kilpisjärvi, northern Finland. Unrooted maximum likelihood tree based on concatenated  
339 alignments of amino acid sequences from 122 archaeal and 120 bacterial single-copy genes.  
340 Additional information about the MAGs can be found in **Suppl. Table S2**.

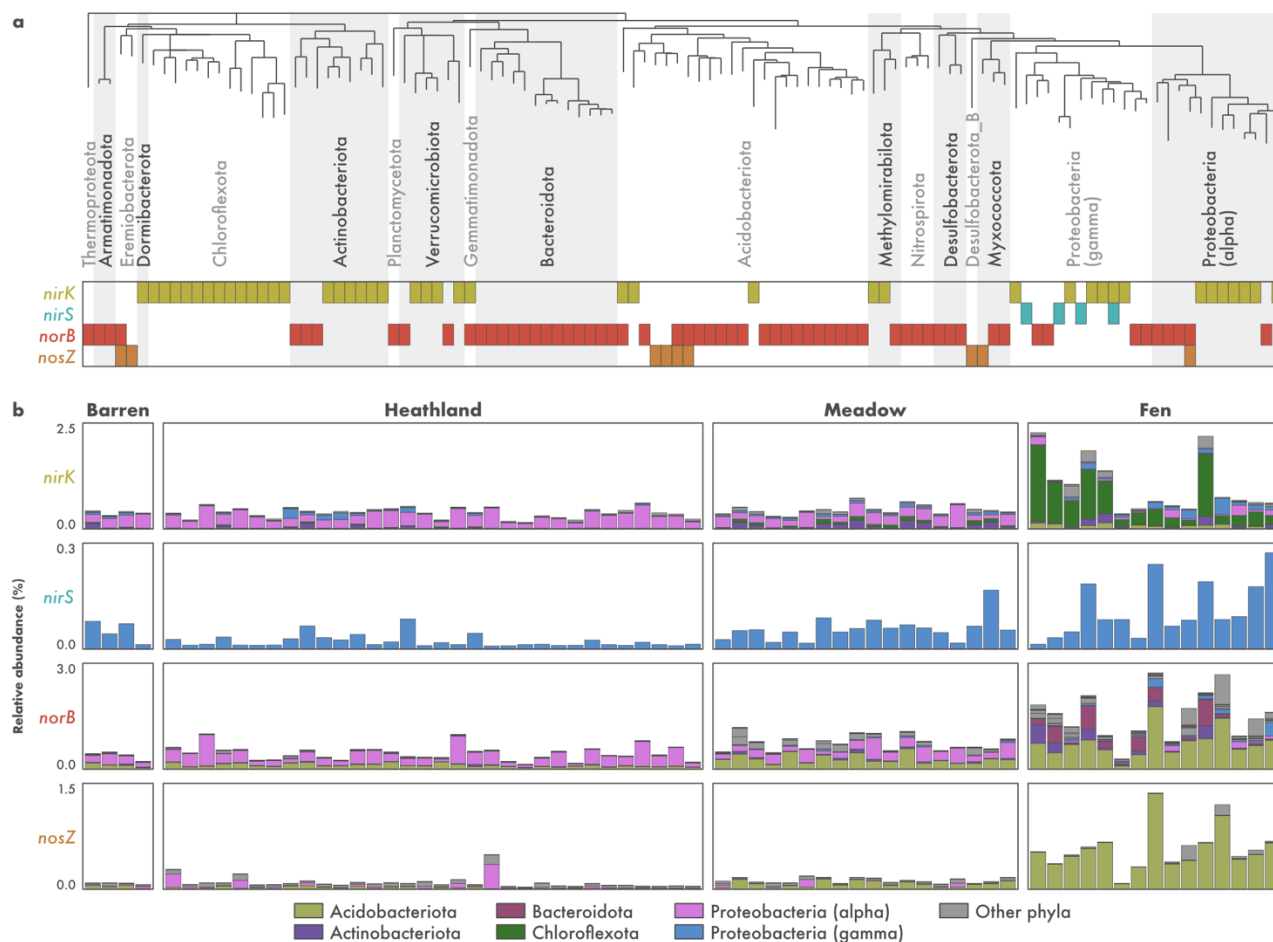


341 **Fig. 2 | Microbial community composition across different soil ecosystems in the**  
342 **tundra.** Relative abundance of 761 non-redundant metagenome-assembled genomes (MAGs)  
343 recovered from soils in Kilpisjärvi, northern Finland. Relative abundances were computed as a  
344 proportion of the reads mapping to each MAG. Phylum-level taxonomic assignments are shown  
345 for the major groups found. The scheme on the top of the figure represents ecosystem-level  
346 methane (CH<sub>4</sub>) and nitrous oxide (N<sub>2</sub>O) fluxes based on *in situ* measurements (**Suppl. Fig. S1**).

### 347 **Microorganisms from tundra soils have truncated denitrification pathways**

348 To gain insights into the microorganisms involved with the cycling of N<sub>2</sub>O in tundra soils, we  
349 traced the curated denitrification genes to the set of recovered MAGs. Denitrification genes were  
350 found in 110 of the 796 MAGs (13.8%) (**Suppl. Table S2**). These were affiliated with the  
351 archaeal phylum Thermoproteota and many bacterial phyla such as Proteobacteria (Gamma-  
352 and Alphaproteobacteria), Acidobacteriota, Bacteroidota, Actinobacteriota, Chloroflexota, and  
353 Verrucomicrobiota (**Fig. 3a**). However, only 17 MAGs were assigned to a validly described  
354 genera (**Suppl. Table S2**). These included members of the Acidobacteriota (*Solibacter*,  
355 *Sulfotelmatobacter*, *Terracidiphilus*, and *Gaiella*), Myxococcota (*Anaeromyxobacter*),  
356 Planctomycetota (*Singulisphaera*), Proteobacteria (Alphaproteobacteria: *Bauldia*,  
357 *Bradyrhizobium*, *Methylocella*, and *Reyranella*; Gammaproteobacteria: *Gallionella* and

358 *Rhizobacter*), and Verrucomicrobiota (*Lacunisphaera* and *Opitutus*). On average, 1.8% of the  
 359 reads in each sample were recruited by all denitrifiers combined (minimum: 0.4%, maximum:  
 360 6.1%).



361 **Fig. 3 | Metabolic potential for denitrification in tundra soils. a)** Distribution of  
 362 denitrification genes across 110 metagenome-assembled genomes (MAGs) recovered from  
 363 tundra soils in Kilpisjärvi, northern Finland. Genes encoding the nitrite (*nirK/nirS*), nitric oxide  
 364 (*norB*), and nitrous oxide (*nosZ*) reductases were annotated using a three-step approach  
 365 including (1) identification using hidden Markov models from the KOfam database, (2) manual  
 366 inspection for the presence of conserved residues at positions associated with the binding of co-  
 367 factors and active sites, and (3) phylogenetic analyses along with sequences from archaeal and  
 368 bacterial genomes (**Suppl. Fig. S5**). **b)** Phylum-level relative abundance of microorganisms  
 369 harbouring denitrification genes across the different soil ecosystems, computed as a proportion  
 370 of reads mapping to each MAG.

371 Genes involved in denitrification were found exclusively in MAGs with truncated denitrification  
 372 pathways, i.e. MAGs missing one or more genes involved in the complete denitrification process

373 **(Fig. 3a)**. Of the 110 MAGs harbouring denitrification genes, the vast majority (n = 104)  
374 encoded only one of the Nir, Nor, and Nos enzymes and no MAG encoded all the three enzymes  
375 required for the reduction of NO<sub>2</sub><sup>-</sup> to N<sub>2</sub>. Unsurprisingly, co-occurrence of genes encoding the  
376 three enzymes was also not observed in any of the other genomic bins of lower quality that were  
377 discarded from the final MAG dataset (i.e. bins that were < 50% complete and/or > 10%  
378 redundant). To verify if microorganisms with truncated denitrification pathways are common  
379 in other tundra systems, we expanded our analysis to 1529 MAGs recovered from permafrost  
380 peatland, bog, and fen soils in Stordalen Mire, northern Sweden [37]. Among these, 225 MAGs  
381 (14.7%) contained denitrification genes (**Suppl. Fig. S4**). MAGs encompassed a similar  
382 taxonomic profile as observed in the Kilpisjärvi dataset, and MAGs with truncated  
383 denitrification pathways were also the norm in Stordalen Mire soils. Only one MAG, assigned  
384 to the Gammaproteobacteria genus *Janthinobacterium*, encoded all the Nir, Nor, and Nos  
385 enzymes required for the reduction of NO<sub>2</sub><sup>-</sup> to N<sub>2</sub>.

### 386 **Microorganisms affiliated with the Chloroflexota lineage Ellin6529 are the** 387 **main denitrifiers *stricto sensu* in fen soils**

388 The reduction of NO<sub>2</sub><sup>-</sup> to NO, performed by microorganisms harbouring the *nirK* or *nirS* genes,  
389 is the hallmark step of denitrification and is often referred to as denitrification *stricto sensu* as  
390 it involves the conversion of a soluble substrate to a gaseous product thus leading to the removal  
391 of N from the system [12]. Of the 110 Kilpisjärvi MAGs harbouring genes involved in  
392 denitrification, 46 contained *nirK/nirS* genes and are thus potential denitrifiers *stricto sensu*  
393 **(Fig. 3a)**. These belonged mainly to the bacterial phyla Chloroflexota, Actinobacteriota, and  
394 Proteobacteria (Alpha- and Gammaproteobacteria). Most MAGs (n = 43) contained the *nirK*  
395 gene, which encodes the copper-containing form of Nir (**Suppl. Fig. S5a**). The *nirS* gene  
396 encoding the cytochrome cd<sub>1</sub>-containing form of Nir was present in four Gammaproteobacteria  
397 MAGs (**Suppl. Fig. S5b**), including one MAG that contained both genes.

398 The composition of potential denitrifier *stricto sensu* communities differed across the ecosystems  
399 **(Fig. 3b)**. MAGs belonging to the Alphaproteobacteria class of the Proteobacteria were the most  
400 abundant in the barren, heathland, and meadow soils, particularly the MAG KUL-0154  
401 assigned to the genera *Bradyrhizobium* (**Suppl. Fig. S6**). Two other Alphaproteobacteria  
402 MAGs that do not correspond to formally described genera in the families Acetobacteraceae and  
403 Beijerinckiaceae (KUL-0057 and KUL-0056, respectively) were also found at high abundances.  
404 In addition, one Actinobacteriota MAG assigned to an uncharacterized genus in the family  
405 Gaiellaceae (KWL-0073), was abundant in the meadow soils. On the other hand, fen

406 communities were dominated by MAGs belonging to the phylum Chloroflexota (**Fig. 3b**), which  
407 included seven MAGs assigned to the class-level lineage Ellin6529 (**Suppl. Fig. S6**).

408 None of the Ellin6529 MAGs contained the key genes involved in autotrophic carbon fixation,  
409 dissimilatory sulfate reduction, dissimilatory nitrate reduction to ammonia, and nitrogen  
410 fixation (**Suppl. Table S3**). Analysis of genes encoding terminal oxidases involved in the  
411 aerobic respiratory electron chain revealed that all seven Ellin6529 MAGs harboured the  
412 *coxABC* genes encoding the *aa3*-type cytochrome c oxidase. Four MAGs also contained the  
413 *cydAB* genes encoding the cytochrome *bd* ubiquinol oxidase, a terminal oxidase with high  
414 affinity for oxygen that also plays a role in preventing the inactivation of oxygen-sensitive  
415 enzymes and protecting against oxidative and nitrosative stress, toxic compounds such as  
416 cyanide, and other stress conditions such as high temperature and high pH [83, 84]. The  
417 dominant MAGs in the barren, heathland, and meadow soils encoded a different set of aerobic  
418 terminal oxidases. In addition to the *cydAB* genes, the MAGs KUL-0057 and KUL-0154 also  
419 contained the *cyoABCD* genes encoding the cytochrome o ubiquinol oxidase, which is the main  
420 terminal oxidase under highly aerobic conditions [85], and KUL-0057 also contained genes  
421 encoding the *cbb3*-type cytochrome c oxidase, a terminal oxidase with high affinity for oxygen  
422 [86]. Genes involved in the Calvin cycle (e.g. *rbcL*, *rbcS*, and *prkB*) were found in the  
423 *Bradyrhizobium* MAG (KUL-0154), and none of the key genes for autotrophic carbon fixation  
424 pathways were present in the other dominant Alphaproteobacteria MAGs.

### 425 **Acidobacteriota with the potential to reduce NO and N<sub>2</sub>O are abundant in the fens**

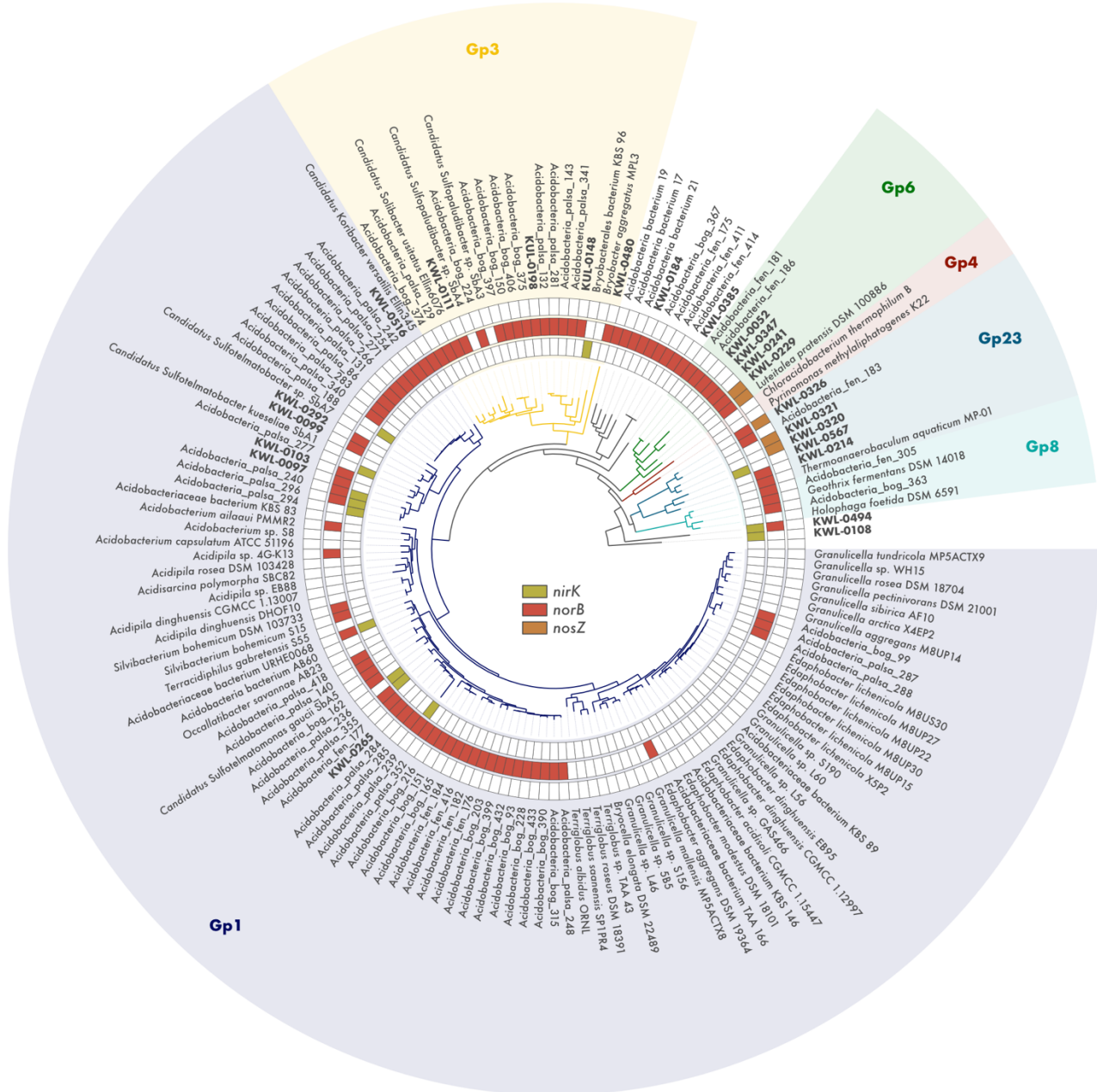
426 The stepwise reduction of NO to N<sub>2</sub>O and N<sub>2</sub> carried out by microorganisms containing the *norB*  
427 and *nosZ* genes, respectively, represents the final step of denitrification and the main biotic  
428 control on N<sub>2</sub>O emissions. Soil denitrification rates depend on multiple environmental  
429 conditions such as adequate moisture and inorganic N availability, but whether it results in the  
430 emission of N<sub>2</sub>O or N<sub>2</sub> is ultimately linked to a balance between the activity of NO and N<sub>2</sub>O  
431 reducers [11, 15]. *norB* and *nosZ* genes were identified in 62 and 9 Kilpisjärvi MAGs,  
432 respectively, belonging mostly to the phyla Actinobacteriota, Bacteroidota, Acidobacteriota, and  
433 Proteobacteria (class Alphaproteobacteria) (**Fig. 3a**). With the exception of one  
434 Gemmatimonadota and one Acidobacteriota MAG, *norB*- and *nosZ*-containing MAGs were  
435 almost exclusively non-denitrifiers *stricto sensu*, i.e. they did not harbour the *nirK/nirS* genes  
436 involved in the reduction of NO<sub>2</sub><sup>-</sup> to NO. Most MAGs (n = 48) harboured a *norB* gene encoding  
437 the monomeric, quinol-dependent form of Nor (qNor), while the remaining MAGs (n = 8) encoded  
438 the cytochrome c-dependent Nor (cNor) (**Suppl. Fig. S5c**). In regards to the *nosZ* gene, most  
439 MAGs (n = 6) contained sequences affiliated with the clade II (also known as atypical) NosZ [14,

440 15, 18] (**Suppl. Fig. S5d**). Only four MAGs contained both the *norB* and *nosZ* genes and thus  
441 have the potential to reduce NO completely to N<sub>2</sub> (**Fig. 3a**).

442 As observed for the denitrifier *stricto sensu* communities, the communities of potential NO and  
443 N<sub>2</sub>O reducers also differed between the ecosystems (**Fig. 3b**). MAGs assigned to the  
444 Alphaproteobacteria class of the Proteobacteria were the most abundant in the barren,  
445 heathland, and meadow soils. In particular, the MAG KWL-0112 assigned to the genera  
446 *Reyranella* was the dominant *norB*-containing MAG, while KUL-0116 (belonging to an  
447 uncharacterized genus in the family Acetobacteraceae) was the dominant MAG harbouring the  
448 *nosZ* gene (**Suppl. Fig. S6**). On the other hand, fen communities were dominated by  
449 Acidobacteriota MAGs (**Fig. 3b**), particularly the *norB*- and *nosZ*-containing MAG KWL-0326  
450 affiliated with the class Thermoanaerobaculia (**Suppl. Fig. S6**). This MAG contained the same  
451 set of genes encoding aerobic terminal oxidases as found in the *nirK*-containing Ellin6529 MAGs  
452 that were dominant in the fen sites, namely *coxABC* and *cydAB* (**Suppl. Table S3**). No genes  
453 involved in carbon fixation, dissimilatory sulfate reduction, dissimilatory nitrate reduction to  
454 ammonia, and nitrogen fixation were found in any of the dominant *norB*- and *nosZ*-containing  
455 MAGs.

456 To elucidate the phylogenetic placement of the Acidobacteriota MAGs and to verify if the  
457 potential for NO and N<sub>2</sub>O reduction is present in other members of this phylum, we included in  
458 our analysis all available genomes of Acidobacteriota strains and candidate taxa available on  
459 GenBank. This revealed that genes encoding the Nir and Nos enzymes are widespread across  
460 the phylum Acidobacteriota (**Fig. 4**). Genes encoding the Nor enzyme were present in all but  
461 one of the six Acidobacteriota subdivisions with genomes from cultured representatives. This  
462 included the strains *Acidobacterium ailaoui* PMMR2 (subdivision Gp1), *Acidipila* sp. 4G-K13  
463 (Gp1), *Silvibacterium bohemicum* DSM 103733 and *S. bohemicum* S15 (Gp1), Acidobacteriaceae  
464 bacterium URHE0068 (Gp1), *Edaphobacter aggregans* DSM 19364 (Gp1), *Luteitalea pratensis*  
465 DSM 100886 (Gp6), *Geothrix fermentans* DSM 14018 (Gp8), and *Thermoanaerobaculum*  
466 *aquaticum* MP-01 (Gp23), as well as the candidate taxa *Candidatus* Koribacter versatilis  
467 Ellin345 (Gp1), *Candidatus* Sulfotelmatomonas gaucii SbA5 (Gp1), and *Candidatus* Solibacter  
468 usitatus Ellin6076 (Gp3). On the other hand, genes encoding the Nos enzyme were found only  
469 in members of the subdivisions Gp6 and Gp23.





470 **Fig. 4 | Metabolic potential for denitrification among members of the phylum**  
 471 **Acidobacteriota.** Phylogenomic analysis of 85 Acidobacteriota metagenome-assembled  
 472 genomes (MAGs) containing denitrification genes recovered from tundra soils in Kilpisjärvi  
 473 (northern Finland) and Stordalen Mire (northern Sweden), and 69 genomes of Acidobacteriota  
 474 strains and candidate taxa. Maximum likelihood tree based on concatenated alignments of 23  
 475 ribosomal proteins and rooted with *Escherichia coli* ATCC 11775 (not shown). Genes encoding  
 476 the nitrite (*nirK*), nitric oxide (*norB*), and nitrous oxide (*nosZ*) reductases were annotated using  
 477 a three-step approach to avoid false positives (see methods).

## 478 Discussion

479 The 796 MAGs obtained in the present study by a manual binning and curation effort represent  
480 one of the largest genomic catalogues of microorganisms from tundra soils to date. Earlier gene-  
481 centric investigations have revealed the potential for complete denitrification in tundra soils  
482 [29, 87], however, these approaches fail to reveal the wider genomic context of the genes involved  
483 in this pathway. By applying the genome-resolved metagenomics approach, we traced  
484 denitrification genes to specific microbial populations, thereby allowing a detailed investigation  
485 of the genomic makeup of potential denitrifiers in tundra soils. This approach also enabled us  
486 to access the genomes of uncultured, poorly characterized taxa, which comprise the majority of  
487 the microorganisms in soils and other complex ecosystems [33, 34]. Our genome-resolved survey  
488 revealed that denitrification across different tundra soil ecosystems is dominated by  
489 microorganisms with truncated denitrification pathways (i.e. harbouring only a subset of the  
490 genes required for complete denitrification), most of which represent poorly characterized taxa  
491 without cultured representatives. With the support of *in situ* measurements of N<sub>2</sub>O fluxes, we  
492 hypothesize that microorganisms with truncated denitrification pathways are important  
493 drivers of N<sub>2</sub>O cycling in tundra soils.

494 The congruence of these findings in both our original dataset of northern Finland soils and a re-  
495 analysis of a comprehensive metagenomic dataset from soils in northern Sweden [37] suggests  
496 that truncated denitrification pathways are not a methodological artifact arising from the  
497 metabolic reconstruction of fragmented genomes. Indeed, recent genome-resolved investigations  
498 have shown that cross-feeding between microorganisms with truncated metabolic pathways,  
499 also known as metabolic handoffs, are the norm across a wide range of ecosystems such as  
500 grassland soil, aquifer sediment, groundwater, and the ocean, and not only in relation to  
501 denitrification but other redox transformations as well [21, 88, 89]. Although it is quite  
502 established that denitrification is a community effort performed by different microbial  
503 populations [12–15], genome-resolved metagenomic studies are beginning to reveal a more in-  
504 depth, ecosystem-centric representation of the denitrification pathway. In addition to their  
505 predominance in genomic databases [14], it appears that truncated denitrifiers are also  
506 dominant within defined ecosystems across various terrestrial and aquatic biomes, including  
507 the tundra. It has been suggested that the partitioning of metabolic pathways across different  
508 populations via metabolic handoffs is advantageous as it eliminates competition between  
509 enzymes accelerating substrate consumption [15, 22] and provides flexibility and resilience to  
510 the communities in face of environmental disturbances [21]. We further hypothesize that the  
511 predominance of denitrification pathways characterized mostly by metabolic handoffs in tundra

512 soils could be related to N limitation. If metabolic handoffs enable a more effective substrate  
513 consumption as previously suggested [15, 22], truncated denitrification pathways would be  
514 favoured in tundra soils which are mostly N limited but undergo rapid surges in N availability  
515 e.g. during the spring melting season [90].

516 Our results showed that denitrifier communities in the tundra differ between drier upland  
517 ecosystems (barren, heathland, and meadow soils) and water-logged fens. This is likely related  
518 to differences in soil moisture affecting oxygen availability in these ecosystems. The dominant  
519 denitrifier populations in the oxic dry upland soils, related to the genera *Bradyrhizobium*,  
520 *Reyranella*, and other uncharacterized genera in the class Alphaproteobacteria, encoded aerobic  
521 terminal oxidases that are active under highly aerobic conditions as well as oxidases with high  
522 oxygen affinity [85, 86]. The former likely provides an adaptive advantage in these soils by  
523 allowing rapid aerobic growth under standard conditions of high oxygen availability, and the  
524 latter would sustain growth in microoxic niches within the soil matrix and during periods of  
525 reduced oxygen availability (e.g. during the spring melting season).

526 On the other hand, fen soils are continuously inundated because the water table is at or near  
527 the soil surface. The result is a mostly anoxic environment due to the slow rate at which oxygen  
528 diffuses into the water-logged soil, favouring reduced rather than oxidized soil chemistry. In  
529 line with this, we found a predominance of anaerobic processes in the fens, including a higher  
530 abundance of genes involved in denitrification, sulfate reduction, and methanogenesis, the  
531 latter supported by *in situ* measurements showing net CH<sub>4</sub> emission at the fen sites.  
532 Communities of potential denitrifiers in the fen soils were dominated by somewhat enigmatic  
533 taxa, namely potential NO<sub>2</sub><sup>-</sup> reducers affiliated with the class Ellin6529 of the Chloroflexota  
534 and NO/N<sub>2</sub>O reducers assigned to the subdivision Gp23 of the Acidobacteriota. Both groups are  
535 major members of microbial communities in soils worldwide [91], and RNA-based investigations  
536 have shown that they are active in tundra soils during both summer and winter seasons [41,  
537 92]. *Thermoanaerobaculum aquaticum* MP-01, the only cultivated member of the  
538 Acidobacteriota subdivision Gp23, is a strictly anaerobic bacterium that has been shown to use  
539 Fe and Mn, but not NO<sub>3</sub><sup>-</sup> nor NO<sub>2</sub><sup>-</sup>, as electron acceptors in anaerobic respiration [93]. However,  
540 studies investigating the use of nitrogen oxides in anaerobic respiration usually provide soluble  
541 NO<sub>3</sub><sup>-</sup> or NO<sub>2</sub><sup>-</sup> as electron acceptors, not the gases NO and N<sub>2</sub>O, which bias against truncated  
542 denitrifiers that do not contain the *narG* and *nirK/nirS* genes [94]. Ellin6529 – formerly G04 –  
543 were first detected by culture-independent methods in alpine tundra wet meadow soil in the  
544 Colorado Rocky Mountains, USA [95], and later isolated in a study targeting slow-growing and  
545 mini-colony forming bacteria from Australian agricultural soil [96]. However, their ecological,  
546 physiological, and metabolic preferences remain largely unknown. Their genomic composition

547 and high abundance in the water-logged, anoxic fen soils suggest that the Ellin6529 and Gp23  
548 populations found in this study are likely able to grow anaerobically with the use of NO and  
549 N<sub>2</sub>O as electron acceptors. However, it is known that in addition to their role in anaerobic  
550 respiration, NO and N<sub>2</sub>O reduction can be used as a detoxification mechanism or as electron  
551 sink for metabolism. For example, the aerobe *Gemmatimonas aurantica* T-27 is not able to grow  
552 on N<sub>2</sub>O alone, but can use N<sub>2</sub>O as electron acceptor transiently when oxygen is depleted [97].

553 In addition to microbial community structure, differences in N<sub>2</sub>O fluxes observed between  
554 upland and fen soils also appear to be linked to soil moisture. Some of the drier upland sites  
555 investigated were hotspots of N<sub>2</sub>O consumption. This is particularly interesting for the acidic  
556 heathland soils, as low pH is known to impair the expression of the NosZ enzyme thus promoting  
557 N<sub>2</sub>O emission [98, 99]. On the other hand, fens had close to net-zero N<sub>2</sub>O fluxes, which is in line  
558 with previous observations for water-saturated soils both in the tundra[7] and worldwide [11,  
559 13]. This has been linked to lower rates of N mineralization and nitrification in anoxic  
560 ecosystems, which limit the availability of NO<sub>3</sub><sup>-</sup> and NO<sub>2</sub><sup>-</sup> and promote complete denitrification,  
561 resulting in N<sub>2</sub> as end product rather than N<sub>2</sub>O. Indeed, supplementing fen soils in the tundra  
562 with NO<sub>3</sub><sup>-</sup> and NO<sub>2</sub><sup>-</sup> has shown to promote N<sub>2</sub>O emissions [100]. Moreover, climate change  
563 models predict lowering of the water table in high-latitude wetlands, which could lead to  
564 increased N<sub>2</sub>O emissions from these ecosystems [101, 102].

## 565 **Conclusions**

566 A better understanding of denitrification is paramount for our ability to model N<sub>2</sub>O emissions  
567 and mitigate climate change. High-latitude environments in particular have experienced  
568 amplified warming in recent decades, a trend that is likely to continue in the coming centuries.  
569 As mechanisms of GHG emissions are very climate sensitive, the contribution of tundra soils to  
570 global GHG atmospheric levels is thus predicted to increase in the future leading to a positive  
571 feedback loop. Compared with carbon dioxide and CH<sub>4</sub>, measurements of N<sub>2</sub>O fluxes in tundra  
572 soils are sparse and are rarely coupled with a characterization of the microorganisms involved,  
573 making the magnitude and drivers of N<sub>2</sub>O fluxes across the polar regions uncertain. While  
574 microorganisms with truncated denitrification pathways appear to dominate the denitrifier  
575 communities investigated here, the potential for complete denitrification was present at the  
576 ecosystem level. In addition to a better monitoring of N<sub>2</sub>O emissions throughout the tundra  
577 biome, our results suggest that a better understanding of the contribution of tundra soil to global  
578 N<sub>2</sub>O levels relies on the elucidation of the regulatory mechanisms of metabolic handoffs in  
579 communities dominated by truncated denitrifiers.

## 580 **Declarations**

### 581 **Ethics approval and consent to participate**

582 Not applicable.

### 583 **Consent for publication**

584 Not applicable.

### 585 **Availability of data and materials**

586 Raw metagenomic data and assembled MAGs have been submitted to the European Nucleotide  
587 Archive (ENA) under the project PRJEB41762. All the code used can be found in  
588 <https://github.com/ArcticMicrobialEcology/Kilpisjarvi-MAGs>.

### 589 **Competing interests**

590 The authors declare that they have no competing interests.

### 591 **Funding**

592 This work was funded by the Academy of Finland (grants 314114 and 335354) and the  
593 University of Helsinki. SV was funded by the Microbiology and Biotechnology Doctoral  
594 Programme (MBDP). AMV was funded by the Academy of Finland (grant 286950), the Otto  
595 Malm Foundation, and the Gordon and Betty Moore Foundation (grant 8414). MEM was  
596 supported by the Academy of Finland (grants 314630 and 317054).

### 597 **Author contributions**

598 JH and ML designed the research; SV and JH performed nucleic acid extraction and  
599 metagenomic library preparation; AMV and MEM designed and performed the GHG flux  
600 measurements and analyses; ISP analysed the data and wrote the manuscript; EER and TOD  
601 contributed with the analyses; all authors contributed to the final version of the manuscript.

### 602 **Acknowledgements**

603 We would like to acknowledge CSC – IT Centre for Science for providing the necessary  
604 computing resources and Kimmo Mattila for IT support; the staff from the Kilpisjärvi Biological  
605 Station, Tanja Orpana, Aino Rutanen, Anniina Sarekoski, Johanna Kerttula, and the members  
606 of the BioGeoClimate Modelling Lab for assistance with fieldwork and soil characterization;  
607 Jillian Banfield and Christina Biasi for helpful discussion; Laura Cappelatti for proof-reading

608 the manuscript; Murat Eren, Sebastian Lücker, Donovan Parks, and Antonios Kioukis for tips,  
609 recommendations, and troubleshooting; and all anonymous reviewers who provided important  
610 insights to the original manuscript.

## 611 **References**

- 612 1. IPCC, editor. *Climate Change 2013: The Physical Science Basis. Contribution of Working*  
613 *Group I to the Fifth Assessment Report of the Intergovernmental Panel on Climate Change.*  
614 Cambridge: Cambridge University Press; 2013. doi:10.1017/CBO9781107415324.
- 615 2. Tian H, Xu R, Canadell JG, Thompson RL, Winiwarter W, Suntharalingam P, et al. A  
616 comprehensive quantification of global nitrous oxide sources and sinks. *Nature*. 2020;586:248–  
617 56.
- 618 3. Repo ME, Susiluoto S, Lind SE, Jokinen S, Elsakov V, Biasi C, et al. Large N<sub>2</sub>O emissions  
619 from cryoturbated peat soil in tundra. *Nat Geosci*. 2009;2:189–92.
- 620 4. Marushchak ME, Pitkämäki A, Koponen H, Biasi C, Seppälä M, Martikainen PJ. Hot spots  
621 for nitrous oxide emissions found in different types of permafrost peatlands. *Glob Change Biol*.  
622 2011;17:2601–14.
- 623 5. Stewart KJ, Grogan P, Coxson DS, Siciliano SD. Topography as a key factor driving  
624 atmospheric nitrogen exchanges in arctic terrestrial ecosystems. *Soil Biol Biochem*. 2014;70:96–  
625 112.
- 626 6. Voigt C, Marushchak ME, Lamprecht RE, Jackowicz-Korczyński M, Lindgren A, Mastepanov  
627 M, et al. Increased nitrous oxide emissions from Arctic peatlands after permafrost thaw. *Proc*  
628 *Natl Acad Sci*. 2017;114:6238–43.
- 629 7. Voigt C, Marushchak ME, Abbott BW, Biasi C, Elberling B, Siciliano SD, et al. Nitrous oxide  
630 emissions from permafrost-affected soils. *Nat Rev Earth Environ*. 2020;1:420–34.
- 631 8. Schuur EAG, McGuire AD, Schädel C, Grosse G, Harden JW, Hayes DJ, et al. Climate change  
632 and the permafrost carbon feedback. *Nature*. 2015;520:171–9.
- 633 9. Hugelius G, Loisel J, Chadburn S, Jackson RB, Jones M, MacDonald G, et al. Large stocks of  
634 peatland carbon and nitrogen are vulnerable to permafrost thaw. *Proc Natl Acad Sci*.  
635 2020;117:20438–46.
- 636 10. Post E, Alley RB, Christensen TR, Macias-Fauria M, Forbes BC, Gooseff MN, et al. The  
637 polar regions in a 2°C warmer world. *Sci Adv*. 2019;5:eaaw9883.

- 638 11. Butterbach-Bahl K, Baggs EM, Dannenmann M, Kiese R, Zechmeister-Boltenstern S.  
639 Nitrous oxide emissions from soils: how well do we understand the processes and their controls?  
640 *Philos Trans R Soc B Biol Sci.* 2013;368:20130122.
- 641 12. Zumft WG. Cell biology and molecular basis of denitrification. *Microbiol Mol Biol Rev*  
642 *MMBR.* 1997;61:533–616.
- 643 13. Wallenstein MD, Myrold DD, Firestone M, Voytek M. Environmental controls on  
644 denitrifying communities and denitrification rates: insights from molecular methods. *Ecol Appl.*  
645 2006;16:2143–52.
- 646 14. Graf DRH, Jones CM, Hallin S. Intergenomic Comparisons Highlight Modularity of the  
647 Denitrification Pathway and Underpin the Importance of Community Structure for N<sub>2</sub>O  
648 Emissions. *PLoS ONE.* 2014;9:e114118.
- 649 15. Hallin S, Philippot L, Löffler FE, Sanford RA, Jones CM. Genomics and Ecology of Novel  
650 N<sub>2</sub>O-Reducing Microorganisms. *Trends Microbiol.* 2018;26:43–55.
- 651 16. Bakken LR, Bergaust L, Liu B, Frostegård Å. Regulation of denitrification at the cellular  
652 level: a clue to the understanding of N<sub>2</sub>O emissions from soils. *Philos Trans R Soc B Biol Sci.*  
653 2012;367:1226–34.
- 654 17. Philippot L, Andert J, Jones CM, Bru D, Hallin S. Importance of denitrifiers lacking the  
655 genes encoding the nitrous oxide reductase for N<sub>2</sub>O emissions from soil: role of denitrifier  
656 diversity for N<sub>2</sub>O fluxes. *Glob Change Biol.* 2011;17:1497–504.
- 657 18. Sanford RA, Wagner DD, Wu Q, Chee-Sanford JC, Thomas SH, Cruz-Garcia C, et al.  
658 Unexpected nondenitrifier nitrous oxide reductase gene diversity and abundance in soils. *Proc*  
659 *Natl Acad Sci.* 2012;109:19709–14.
- 660 19. Jones CM, Graf DR, Bru D, Philippot L, Hallin S. The unaccounted yet abundant nitrous  
661 oxide-reducing microbial community: a potential nitrous oxide sink. *ISME J.* 2013;7:417–26.
- 662 20. Jones CM, Spor A, Brennan FP, Breuil M-C, Bru D, Lemanceau P, et al. Recently identified  
663 microbial guild mediates soil N<sub>2</sub>O sink capacity. *Nat Clim Change.* 2014;4:801–5.
- 664 21. Anantharaman K, Brown CT, Hug LA, Sharon I, Castelle CJ, Probst AJ, et al. Thousands  
665 of microbial genomes shed light on interconnected biogeochemical processes in an aquifer  
666 system. *Nat Commun.* 2016;7:13219.
- 667 22. Lilja EE, Johnson DR. Segregating metabolic processes into different microbial cells  
668 accelerates the consumption of inhibitory substrates. *ISME J.* 2016;10:1568–78.

- 669 23. Liu X-Y, Koba K, Koyama LA, Hobbie SE, Weiss MS, Inagaki Y, et al. Nitrate is an important  
670 nitrogen source for Arctic tundra plants. *Proc Natl Acad Sci*. 2018;115:3398–403.
- 671 24. Kou D, Yang G, Li F, Feng X, Zhang D, Mao C, et al. Progressive nitrogen limitation across  
672 the Tibetan alpine permafrost region. *Nat Commun*. 2020;11:3331.
- 673 25. Yergeau E, Kang S, He Z, Zhou J, Kowalchuk GA. Functional microarray analysis of  
674 nitrogen and carbon cycling genes across an Antarctic latitudinal transect. *ISME J*. 2007;1:163–  
675 79.
- 676 26. Yergeau E, Hogues H, Whyte LG, Greer CW. The functional potential of high Arctic  
677 permafrost revealed by metagenomic sequencing, qPCR and microarray analyses. *ISME J*.  
678 2010;4:1206–14.
- 679 27. Palmer K, Biasi C, Horn MA. Contrasting denitrifier communities relate to contrasting N<sub>2</sub>O  
680 emission patterns from acidic peat soils in arctic tundra. *ISME J*. 2012;6:1058–77.
- 681 28. Dai H-T, Zhu R-B, Sun B-W, Che C-S, Hou L-J. Effects of Sea Animal Activities on Tundra  
682 Soil Denitrification and nirS- and nirK-Encoding Denitrifier Community in Maritime  
683 Antarctica. *Front Microbiol*. 2020;11:573302.
- 684 29. Ortiz M, Bosch J, Coclet C, Johnson J, Lebre P, Salawu-Rotimi A, et al. Microbial Nitrogen  
685 Cycling in Antarctic Soils. *Microorganisms*. 2020;8:1442.
- 686 30. Brummell ME, Farrell RE, Siciliano SD. Greenhouse gas soil production and surface fluxes  
687 at a high arctic polar oasis. *Soil Biol Biochem*. 2012;52:1–12.
- 688 31. Chapuis-Lardy L, Wrage N, Metay A, Chotte J-L, Bernoux M. Soils, a sink for N<sub>2</sub>O? A  
689 review. *Glob Change Biol*. 2007;13:1–17.
- 690 32. Yu T, Zhuang Q. Quantifying global N<sub>2</sub>O emissions from natural ecosystem soils using trait-  
691 based biogeochemistry models. *Biogeosciences*. 2019;16:207–22.
- 692 33. Rappé MS, Giovannoni SJ. The Uncultured Microbial Majority. *Annu Rev Microbiol*.  
693 2003;57:369–94.
- 694 34. Steen AD, Crits-Christoph A, Carini P, DeAngelis KM, Fierer N, Lloyd KG, et al. High  
695 proportions of bacteria and archaea across most biomes remain uncultured. *ISME J*.  
696 2019;13:3126–30.
- 697 35. Mackelprang R, Waldrop MP, DeAngelis KM, David MM, Chavarria KL, Blazewicz SJ, et  
698 al. Metagenomic analysis of a permafrost microbial community reveals a rapid response to thaw.  
699 *Nature*. 2011;480:368–71.



- 700 36. Hultman J, Waldrop MP, Mackelprang R, David MM, McFarland J, Blazewicz SJ, et al.  
701 Multi-omics of permafrost, active layer and thermokarst bog soil microbiomes. *Nature*.  
702 2015;521:208–12.
- 703 37. Woodcroft BJ, Singleton CM, Boyd JA, Evans PN, Emerson JB, Zayed AAF, et al. Genome-  
704 centric view of carbon processing in thawing permafrost. *Nature*. 2018;560:49–54.
- 705 38. Pirinen P, Simola H, Aalto J, Kaukoranta J-P, Karlsson P, Ruuhela R. Climatological  
706 statistics of Finland 1981–2010. Helsinki: Finnish Meteorological Institute; 2012.
- 707 39. le Roux PC, Aalto J, Luoto M. Soil moisture’s underestimated role in climate change impact  
708 modelling in low-energy systems. *Glob Change Biol*. 2013;19:2965–75.
- 709 40. Niittynen P, Heikkinen RK, Aalto J, Guisan A, Kemppinen J, Luoto M. Fine-scale tundra  
710 vegetation patterns are strongly related to winter thermal conditions. *Nat Clim Change*. 2020.  
711 doi:10.1038/s41558-020-00916-4.
- 712 41. Viitamäki S, Pessi IS, Virkkala A-M, Niittynen P, Kemppinen J, Eronen-Rasimus E, et al.  
713 The activity and functions of subarctic soil microbial communities vary across vegetation types.  
714 *bioRxiv*. 2021. doi:10.1101/2021.06.12.448001.
- 715 42. le Roux PC, Pellissier L, Wisz MS, Luoto M. Incorporating dominant species as proxies for  
716 biotic interactions strengthens plant community models. *J Ecol*. 2014;102:767–75.
- 717 43. Kemppinen J, Niittynen P, Aalto J, le Roux PC, Luoto M. Water as a resource, stress and  
718 disturbance shaping tundra vegetation. *Oikos*. 2019;128:811–22.
- 719 44. Livingston GP, Hutchinson GL. Enclosure-based measurement of trace gas exchange:  
720 applications and sources of error. In: *Biogenic trace gases: Measuring emissions from soil and*  
721 *water*. Oxford, United Kingdom: Blackwell Science. p. 14–51.
- 722 45. R Core Team. *R: A language and environment for statistical computing*. 2020.
- 723 46. Andrews S. *FastQC: A Quality Control Tool for High Throughput Sequence Data*. 2019.  
724 <http://www.bioinformatics.babraham.ac.uk/projects/fastqc/>.
- 725 47. Ewels P, Magnusson M, Lundin S, Käller M. MultiQC: summarize analysis results for  
726 multiple tools and samples in a single report. *Bioinformatics*. 2016;32:3047–8.
- 727 48. Martin M. Cutadapt removes adapter sequences from high-throughput sequencing reads.  
728 *EMBnet.journal*. 2011;17:10.
- 729 49. Leger A, Leonardi T. *pycoQC, interactive quality control for Oxford Nanopore Sequencing*.  
730 *J Open Source Softw*. 2019;4:1236.

- 731 50. Wick RR. Porechop. 2018. <https://github.com/rrwick/Porechop>.
- 732 51. Li H. seqtk. 2018. <https://github.com/lh3/seqtk>.
- 733 52. Bengtsson-Palme J, Hartmann M, Eriksson KM, Pal C, Thorell K, Larsson DGJ, et al.  
734 METAXA 2: improved identification and taxonomic classification of small and large subunit  
735 rRNA in metagenomic data. *Mol Ecol Resour.* 2015;15:1403–14.
- 736 53. Quast C, Pruesse E, Yilmaz P, Gerken J, Schweer T, Yarza P, et al. The SILVA ribosomal  
737 RNA gene database project: improved data processing and web-based tools. *Nucleic Acids Res.*  
738 2012;41:D590–6.
- 739 54. Schloss PD, Westcott SL, Ryabin T, Hall JR, Hartmann M, Hollister EB, et al. Introducing  
740 mothur: Open-Source, Platform-Independent, Community-Supported Software for Describing  
741 and Comparing Microbial Communities. *Appl Environ Microbiol.* 2009;75:7537–41.
- 742 55. Wang Q, Garrity GM, Tiedje JM, Cole JR. Naïve Bayesian Classifier for Rapid Assignment  
743 of rRNA Sequences into the New Bacterial Taxonomy. *Appl Environ Microbiol.* 2007;73:5261–  
744 7.
- 745 56. Oksanen J, Blanchet FG, Friendly M, Kindt R, Legendre P, McGlenn D, et al. vegan:  
746 Community Ecology Package. 2019. <https://CRAN.R-project.org/package=vegan>.
- 747 57. Li D, Liu C-M, Luo R, Sadakane K, Lam T-W. MEGAHIT: an ultra-fast single-node solution  
748 for large and complex metagenomics assembly via succinct de Bruijn graph. *Bioinformatics.*  
749 2015;31:1674–6.
- 750 58. Kolmogorov M, Bickhart DM, Behsaz B, Gurevich A, Rayko M, Shin SB, et al. metaFlye:  
751 scalable long-read metagenome assembly using repeat graphs. *Nat Methods.* 2020.  
752 doi:10.1038/s41592-020-00971-x.
- 753 59. Langmead B, Salzberg SL. Fast gapped-read alignment with Bowtie 2. *Nat Methods.*  
754 2012;9:357–9.
- 755 60. Li H, Handsaker B, Wysoker A, Fennell T, Ruan J, Homer N, et al. The Sequence  
756 Alignment/Map format and SAMtools. *Bioinformatics.* 2009;25:2078–9.
- 757 61. Walker BJ, Abeel T, Shea T, Priest M, Abouelliel A, Sakthikumar S, et al. Pilon: An  
758 Integrated Tool for Comprehensive Microbial Variant Detection and Genome Assembly  
759 Improvement. *PLoS ONE.* 2014;9:e112963.
- 760 62. Mikheenko A, Saveliev V, Gurevich A. MetaQUAST: evaluation of metagenome assemblies.  
761 *Bioinformatics.* 2016;32:1088–90.

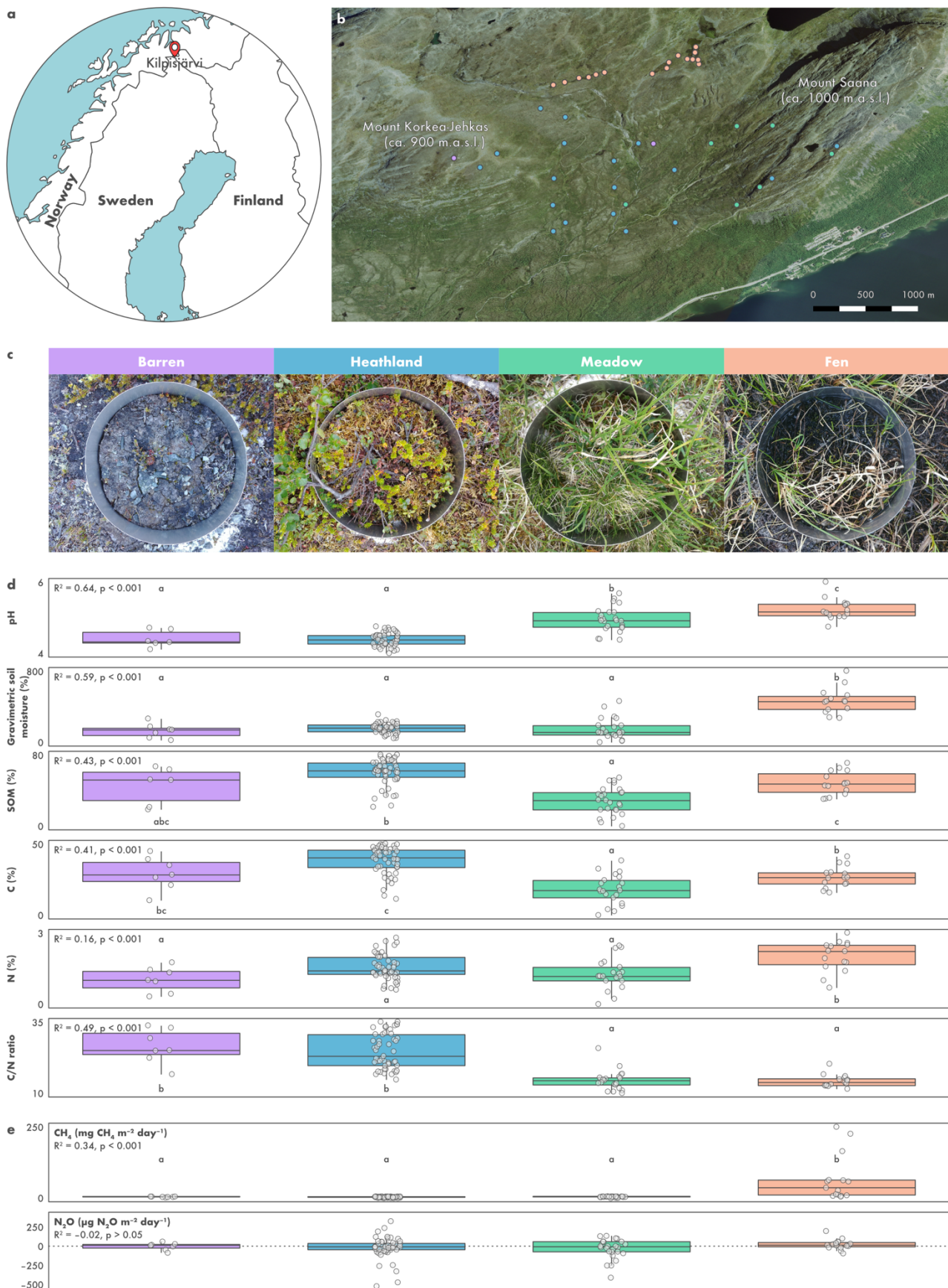
- 762 63. Eren AM, Esen ÖC, Quince C, Vineis JH, Morrison HG, Sogin ML, et al. Anvi'o: an advanced  
763 analysis and visualization platform for 'omics data. *PeerJ*. 2015;3:e1319.
- 764 64. Hyatt D, Chen G-L, LoCascio PF, Land ML, Larimer FW, Hauser LJ. Prodigal: prokaryotic  
765 gene recognition and translation initiation site identification. *BMC Bioinformatics*.  
766 2010;11:119.
- 767 65. Eddy SR. Accelerated Profile HMM Searches. *PLoS Comput Biol*. 2011;7:e1002195.
- 768 66. Buchfink B, Xie C, Huson DH. Fast and sensitive protein alignment using DIAMOND. *Nat*  
769 *Methods*. 2015;12:59–60.
- 770 67. Parks DH, Chuvochina M, Waite DW, Rinke C, Skarszewski A, Chaumeil P-A, et al. A  
771 standardized bacterial taxonomy based on genome phylogeny substantially revises the tree of  
772 life. *Nat Biotechnol*. 2018;36:996–1004.
- 773 68. Parks DH, Chuvochina M, Chaumeil P-A, Rinke C, Mussig AJ, Hugenholtz P. A complete  
774 domain-to-species taxonomy for Bacteria and Archaea. *Nat Biotechnol*. 2020.  
775 doi:10.1038/s41587-020-0501-8.
- 776 69. Alneberg J, Bjarnason BS, de Bruijn I, Schirmer M, Quick J, Ijaz UZ, et al. Binning  
777 metagenomic contigs by coverage and composition. *Nat Methods*. 2014;11:1144–6.
- 778 70. Aramaki T, Blanc-Mathieu R, Endo H, Ohkubo K, Kanehisa M, Goto S, et al. KofamKOALA:  
779 KEGG Ortholog assignment based on profile HMM and adaptive score threshold.  
780 *Bioinformatics*. 2020;36:2251–2.
- 781 71. Katoh K, Standley DM. MAFFT Multiple Sequence Alignment Software Version 7:  
782 Improvements in Performance and Usability. *Mol Biol Evol*. 2013;30:772–80.
- 783 72. Okonechnikov K, Golosova O, Fursov M. Unipro UGENE: a unified bioinformatics toolkit.  
784 *Bioinformatics*. 2012;28:1166–7.
- 785 73. Decleyre H, Heylen K, Tytgat B, Willems A. Highly diverse nirK genes comprise two major  
786 clades that harbour ammonium-producing denitrifiers. *BMC Genomics*. 2016;17:155.
- 787 74. Li Y, Bali S, Borg S, Katzmann E, Ferguson SJ, Schuler D. Cytochrome cd1 Nitrite  
788 Reductase NirS Is Involved in Anaerobic Magnetite Biomineralization in *Magnetospirillum*  
789 *gryphiswaldense* and Requires NirN for Proper d1 Heme Assembly. *J Bacteriol*. 2013;195:4297–  
790 309.
- 791 75. Heylen K, Keltjens J. Redundancy and modularity in membrane-associated dissimilatory  
792 nitrate reduction in *Bacillus*. *Front Microbiol*. 2012;3. doi:10.3389/fmicb.2012.00371.

- 793 76. Price MN, Dehal PS, Arkin AP. FastTree 2 – Approximately Maximum-Likelihood Trees for  
794 Large Alignments. PLoS ONE. 2010;5:e9490.
- 795 77. Woodcroft BJ. CoverM. 2021.
- 796 78. Li H. Minimap and miniasm: fast mapping and de novo assembly for noisy long sequences.  
797 Bioinformatics. 2016;32:2103–10.
- 798 79. Chaumeil P-A, Mussig AJ, Hugenholtz P, Parks DH. GTDB-Tk: a toolkit to classify genomes  
799 with the Genome Taxonomy Database. Bioinformatics. 2019;:btz848.
- 800 80. Edgar RC. MUSCLE: multiple sequence alignment with high accuracy and high throughput.  
801 Nucleic Acids Res. 2004;32:1792–7.
- 802 81. Zhang H, Yohe T, Huang L, Entwistle S, Wu P, Yang Z, et al. dbCAN2: a meta server for  
803 automated carbohydrate-active enzyme annotation. Nucleic Acids Res. 2018;46:W95–101.
- 804 82. Jain C, Rodriguez-R LM, Phillippy AM, Konstantinidis KT, Aluru S. High throughput ANI  
805 analysis of 90K prokaryotic genomes reveals clear species boundaries. Nat Commun.  
806 2018;9:5114.
- 807 83. Borisov VB, Gennis RB, Hemp J, Verkhovsky MI. The cytochrome bd respiratory oxygen  
808 reductases. Biochim Biophys Acta BBA - Bioenerg. 2011;1807:1398–413.
- 809 84. Giuffrè A, Borisov VB, Arese M, Sarti P, Forte E. Cytochrome bd oxidase and bacterial  
810 tolerance to oxidative and nitrosative stress. Biochim Biophys Acta BBA - Bioenerg.  
811 2014;1837:1178–87.
- 812 85. Dinamarca MA, Ruiz-Manzano A, Rojo F. Inactivation of Cytochrome *o* Ubiquinol Oxidase  
813 Relieves Catabolic Repression of the *Pseudomonas putida* GPo1 Alkane Degradation Pathway.  
814 J Bacteriol. 2002;184:3785–93.
- 815 86. Bueno E, Mesa S, Bedmar EJ, Richardson DJ, Delgado MJ. Bacterial Adaptation of  
816 Respiration from Oxidic to Microoxidic and Anoxic Conditions: Redox Control. Antioxid Redox  
817 Signal. 2012;16:819–52.
- 818 87. Makhalanyane TP, Van Goethem MW, Cowan DA. Microbial diversity and functional  
819 capacity in polar soils. Curr Opin Biotechnol. 2016;38:159–66.
- 820 88. Diamond S, Andeer PF, Li Z, Crits-Christoph A, Burstein D, Anantharaman K, et al.  
821 Mediterranean grassland soil C–N compound turnover is dependent on rainfall and depth, and  
822 is mediated by genomically divergent microorganisms. Nat Microbiol. 2019;4:1356–67.

- 823 89. Sun X, Ward BB. Novel metagenome-assembled genomes involved in the nitrogen cycle from  
824 a Pacific oxygen minimum zone. *ISME Commun.* 2021;1:26.
- 825 90. Westergaard-Nielsen A, Balstrøm T, Treier UA, Normand S, Elberling B. Estimating  
826 meltwater retention and associated nitrate redistribution during snowmelt in an Arctic tundra  
827 landscape. *Environ Res Lett.* 2020;15:034025.
- 828 91. Delgado-Baquerizo M, Oliverio AM, Brewer TE, Benavent-González A, Eldridge DJ,  
829 Bardgett RD, et al. A global atlas of the dominant bacteria found in soil. *Science.* 2018;359:320–  
830 5.
- 831 92. Männistö MK, Kurhela E, Tiirola M, Häggblom MM. Acidobacteria dominate the active  
832 bacterial communities of Arctic tundra with widely divergent winter-time snow accumulation  
833 and soil temperatures. *FEMS Microbiol Ecol.* 2013;84:47–59.
- 834 93. Losey NA, Stevenson BS, Busse H-J, Damsté JSS, Rijpstra WIC, Rudd S, et al.  
835 *Thermoanaerobaculum aquaticum* gen. nov., sp. nov., the first cultivated member of  
836 Acidobacteria subdivision 23, isolated from a hot spring. *Int J Syst Evol Microbiol.* 2013;63  
837 Pt\_11:4149–57.
- 838 94. Lycus P, Lovise Bøthun K, Bergaust L, Peele Shapleigh J, Reier Bakken L, Frostegård Å.  
839 Phenotypic and genotypic richness of denitrifiers revealed by a novel isolation strategy. *ISME*  
840 *J.* 2017;11:2219–32.
- 841 95. Costello EK, Schmidt SK. Microbial diversity in alpine tundra wet meadow soil: novel  
842 Chloroflexi from a cold, water-saturated environment. *Environ Microbiol.* 2006;8:1471–86.
- 843 96. Davis KER, Sangwan P, Janssen PH. Acidobacteria, Rubrobacteridae and Chloroflexi are  
844 abundant among very slow-growing and mini-colony-forming soil bacteria. *Environ Microbiol.*  
845 2011;13:798–805.
- 846 97. Park D, Kim H, Yoon S. Nitrous Oxide Reduction by an Obligate Aerobic Bacterium,  
847 *Gemmatimonas aurantiaca* Strain T-27. *Appl Environ Microbiol.* 2017;83.  
848 doi:10.1128/AEM.00502-17.
- 849 98. Liu B, Frostegård Å, Bakken LR. Impaired Reduction of N<sub>2</sub>O to N<sub>2</sub> in Acid Soils Is Due to  
850 a Posttranscriptional Interference with the Expression of *nosZ*. *mBio.* 2014;5.  
851 doi:10.1128/mBio.01383-14.
- 852 99. Samad MS, Biswas A, Bakken LR, Clough TJ, de Klein CAM, Richards KG, et al.  
853 Phylogenetic and functional potential links pH and N<sub>2</sub>O emissions in pasture soils. *Sci Rep.*  
854 2016;6:35990.

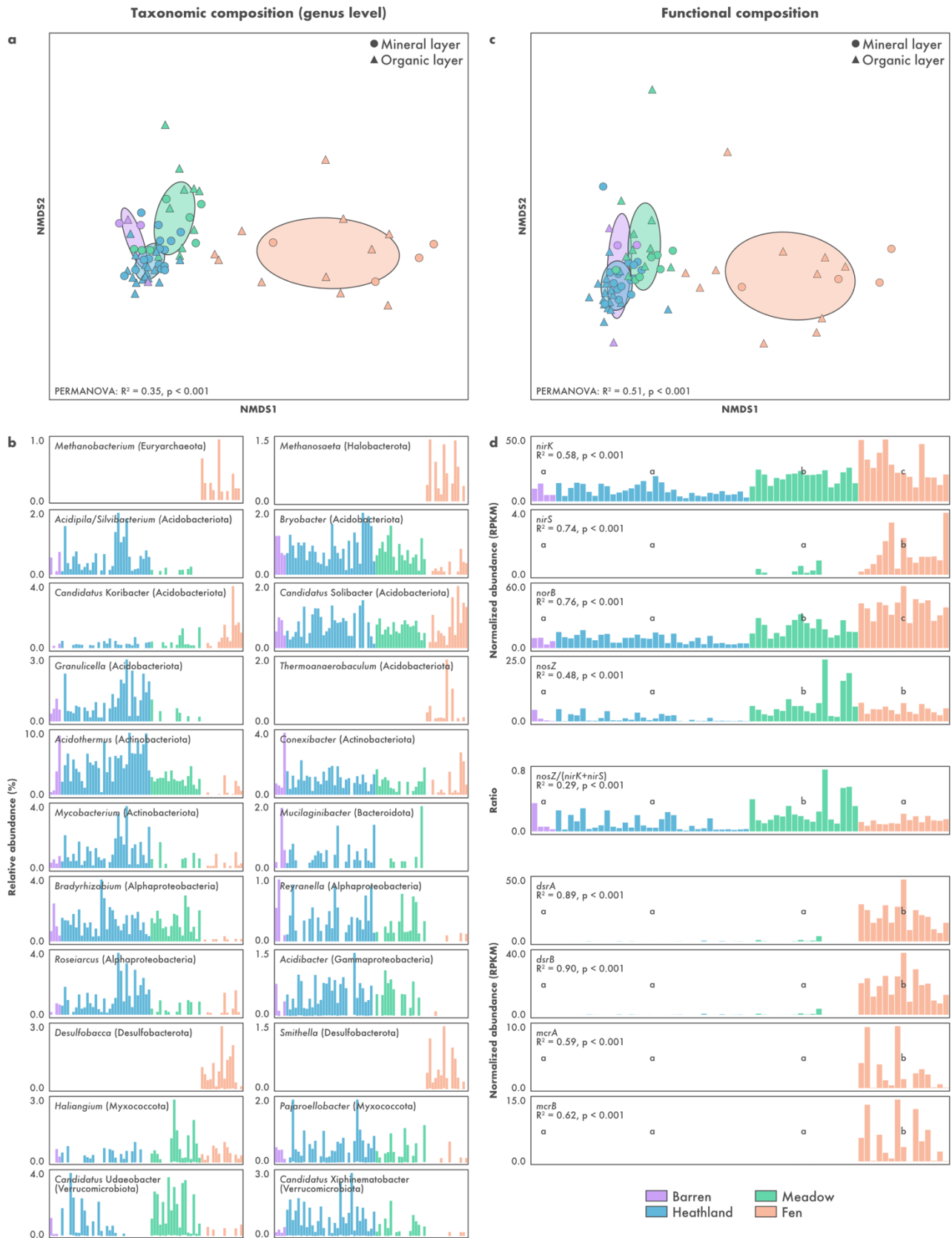
- 855 100. Palmer K, Horn MA. Denitrification Activity of a Remarkably Diverse Fen Denitrifier  
856 Community in Finnish Lapland Is N-Oxide Limited. PLOS ONE. 2015;10:e0123123.
- 857 101. Smith K. The potential for feedback effects induced by global warming on emissions of  
858 nitrous oxide by soils. Glob Change Biol. 1997;3:327–38.
- 859 102. Kåresdotter E, Destouni G, Ghajarnia N, Hugelius G, Kalantari Z. Mapping the  
860 Vulnerability of Arctic Wetlands to Global Warming. Earths Future. 2021;9.  
861 doi:10.1029/2020EF001858.

862 **Supplementary Figures**

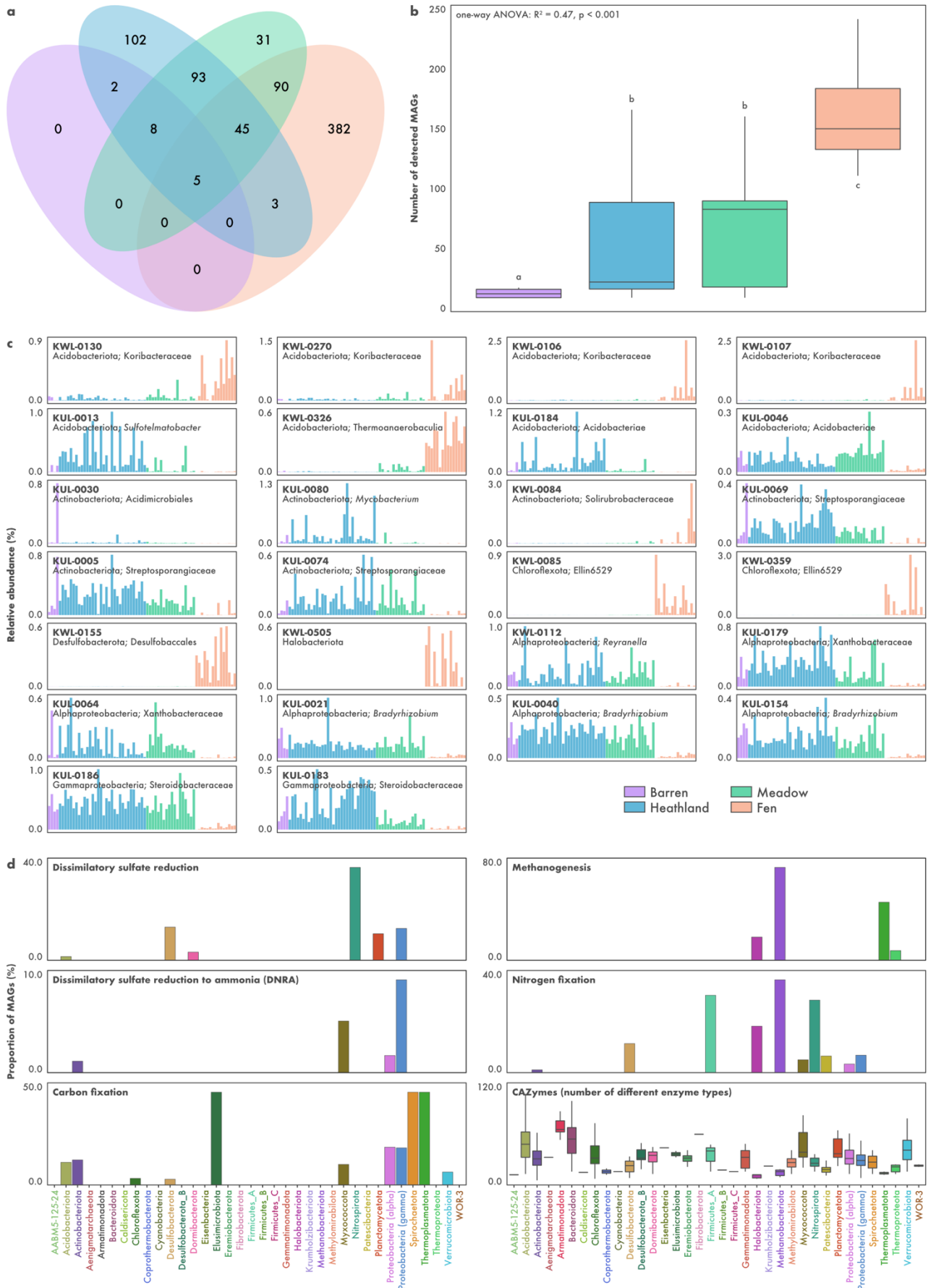


863 **(Previous page) Suppl. Fig. S1 | Saana Nature Reserve, an area of mountain tundra**  
864 **in Kilpisjärvi, northern Finland. a)** Map of Fennoscandia showing the location of Kilpisjärvi.  
865 **b)** Aerial overview of the study area showing the location of the 43 sites sampled for  
866 metagenomic analysis. Image provided by the National Land Survey of Finland under the  
867 Creative Commons CC BY 4.0 license. **c)** Pictures of the four types of soil ecosystems  
868 investigated. **d)** Physicochemical characterization of the soil ecosystems based on an extended  
869 set of 228 samples taken from the organic layer. **e)** *In situ* ecosystem-level nitrous oxide (N<sub>2</sub>O)  
870 and methane (CH<sub>4</sub>) fluxes measured from 101 sites using a static, non-steady state, non-flow-  
871 through system. Negative values represent net uptake and positive net emissions. For clarity,  
872 one outlier measurement from a meadow site (660 μg N<sub>2</sub>O m<sup>-2</sup> day<sup>-1</sup>) was removed.



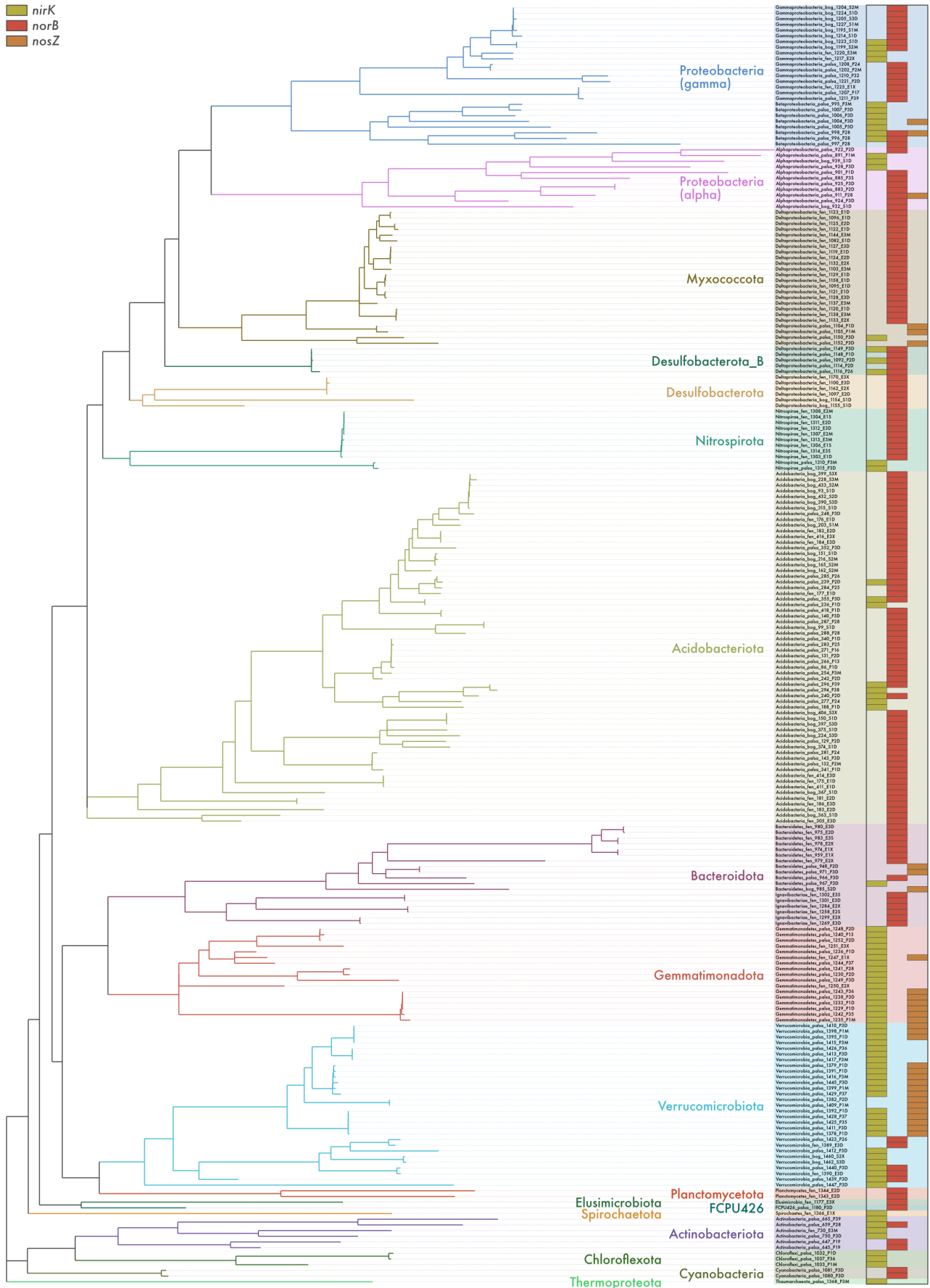


873 **(Previous page) Suppl. Fig. S2 | The microbial diversity of Kilpisjärvi soils as seen**  
874 **using a read-based gene-centric approach.** Taxonomic composition was computed based on  
875 the annotation of unassembled SSU rRNA gene sequences against the SILVA database.  
876 Functional annotation was done by searching assembled genes against the KOfam database.  
877 The annotation of putative denitrification genes was confirmed using a phylogenetic approach.  
878 **a, c)** Non-metric multidimensional scaling (NMDS) of taxonomic and functional community  
879 structure, respectively. Differences between the ecosystems were assessed using permutational  
880 ANOVA (PERMANOVA). **b)** Abundance profile of the five most abundant genera in each  
881 ecosystem. **d)** Abundance profile of marker genes for denitrification, sulfate reduction, and  
882 methanogenesis.



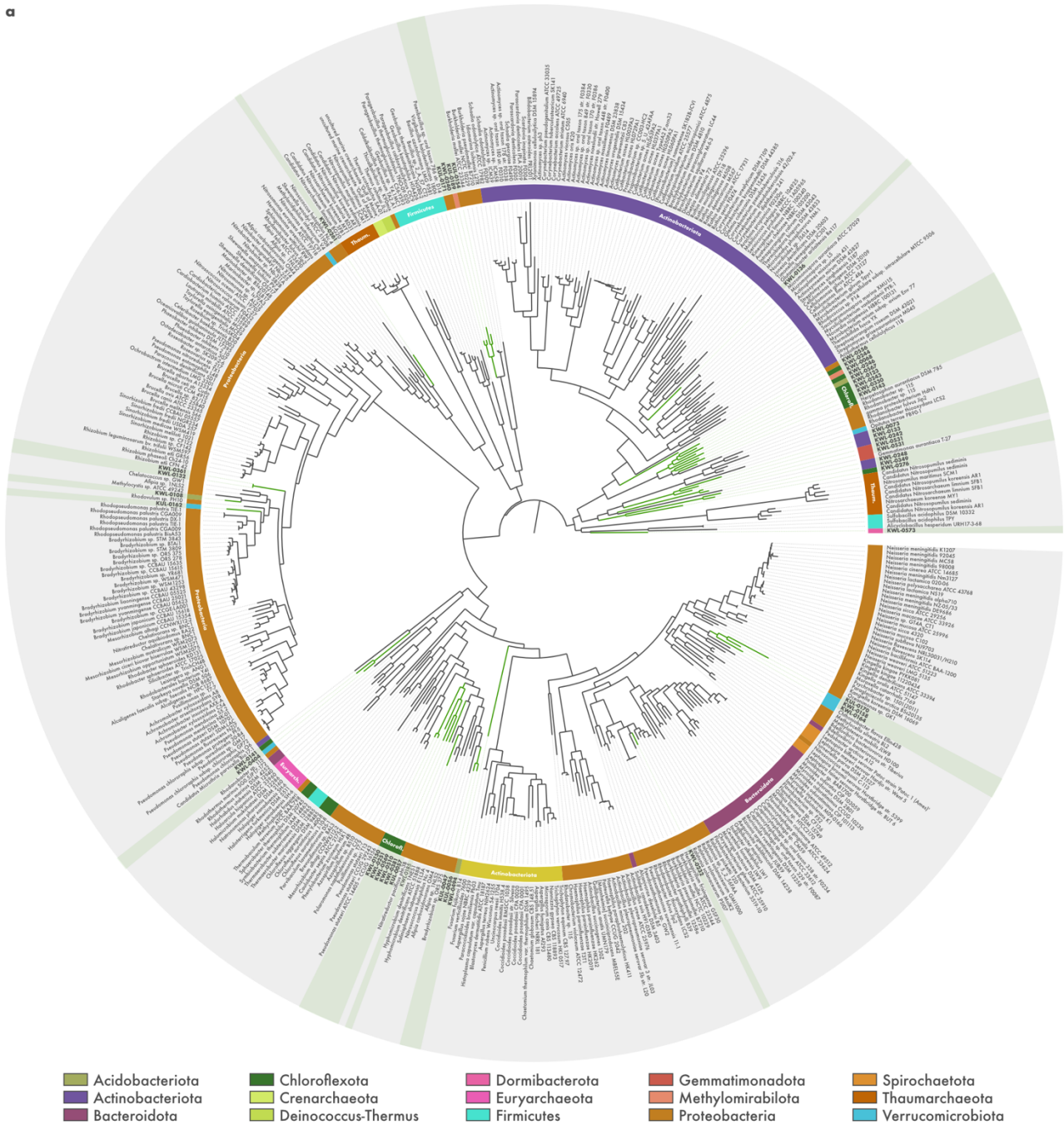
883 **(Previous page) Suppl. Fig. S3 | Overview of the microbial diversity in Kilpisjärvi**  
884 **soils based on a genome-resolved approach. a)** Number of metagenome-assembled  
885 genomes (MAGs) shared between the different ecosystems. **b)** Number of detected MAGs across  
886 the ecosystems. **c)** Relative abundance of the ten most abundant MAGs in each ecosystem,  
887 computed as a proportion of reads mapping to each MAG. **d)** Metabolic potential of the MAGs  
888 based on the annotation of genes against the KOfam database. Barplots represent the  
889 proportion of MAGs in each phylum with complete pathways, i.e. containing  $\geq 75\%$  of the genes  
890 in the pathway. Boxplots of carbohydrate-active enzymes (CAZymes) show the number of  
891 different enzyme types identified in each MAG.

■ *nirK*  
■ *norB*  
■ *nosZ*



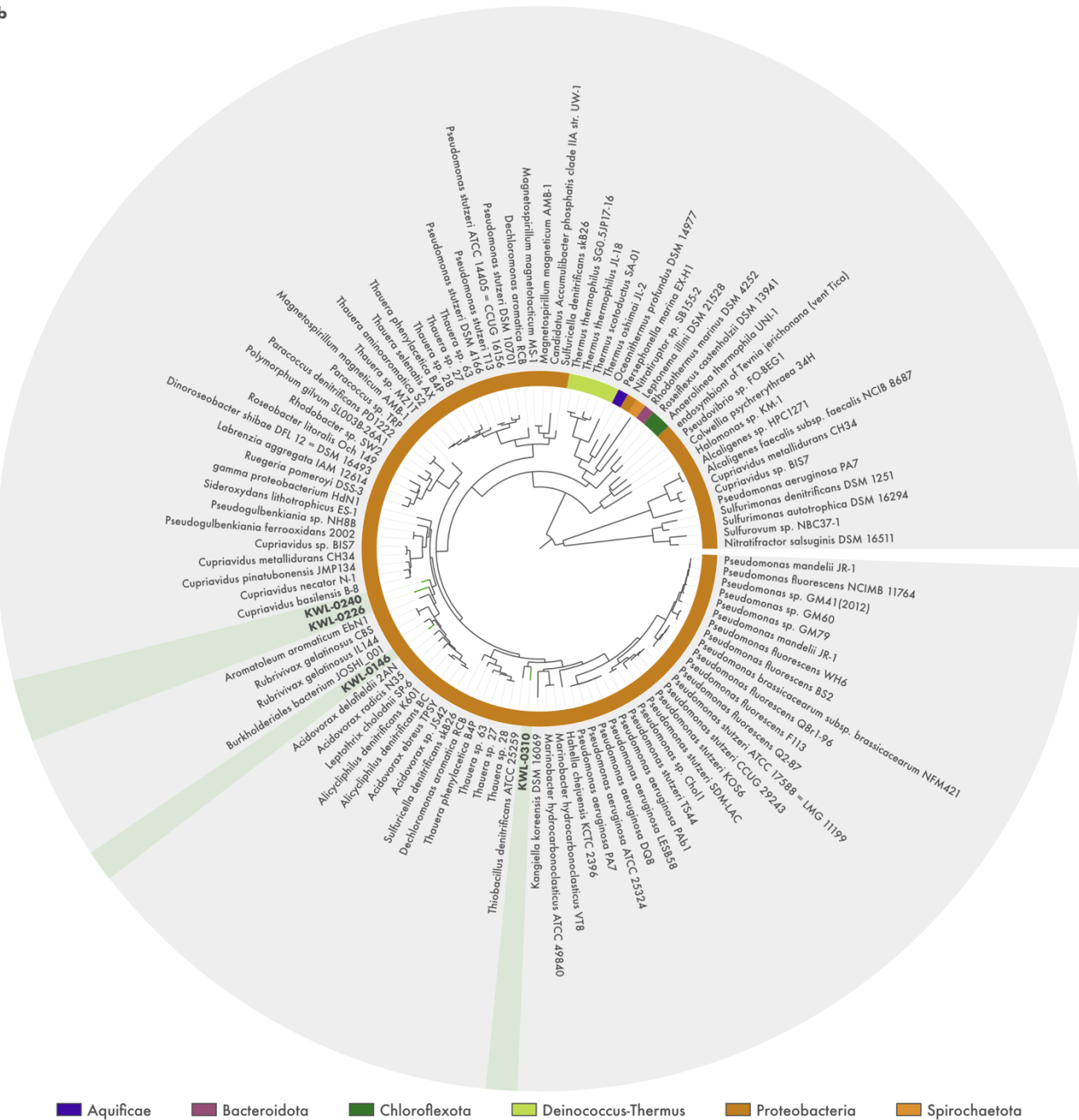
892 **(Previous page) Suppl. Fig. S4 | Metabolic potential for denitrification in Stordalen**  
893 **Mire soils.** Distribution of denitrification genes across 225 metagenome-assembled genomes  
894 (MAGs) from permafrost peatland, bog, and fen soils in Stordalen Mire, northern Sweden. Genes  
895 encoding the nitrite (*nirK*), nitric oxide (*norB*), and nitrous oxide (*nosZ*) reductases were  
896 annotated using a three-step approach including (1) identification using hidden Markov models  
897 from the KOfam database, (2) manual inspection for the presence of conserved residues at  
898 positions associated with the binding of co-factors and active sites, and (3) phylogenetic analyses  
899 along with sequences from archaeal and bacterial genomes. Phylogenomic analysis of MAGs  
900 was done based on concatenated alignments of amino acid sequences from 122 archaeal and 120  
901 bacterial single-copy genes.

a



902 **Suppl. Fig. S5 | Phylogeny of a) *nirK*, b) *nirS*, c) *norB*, and d) *nosZ* sequences from**  
 903 **metagenome-assembled genomes (MAGs) recovered from tundra soils in Kilpisjärvi,**  
 904 **northern Finland.** Midpoint-rooted maximum-likelihood trees of translated sequences from  
 905 Kilpisjärvi MAGs (highlighted) along with reference sequences from archaeal and bacterial  
 906 genomes.

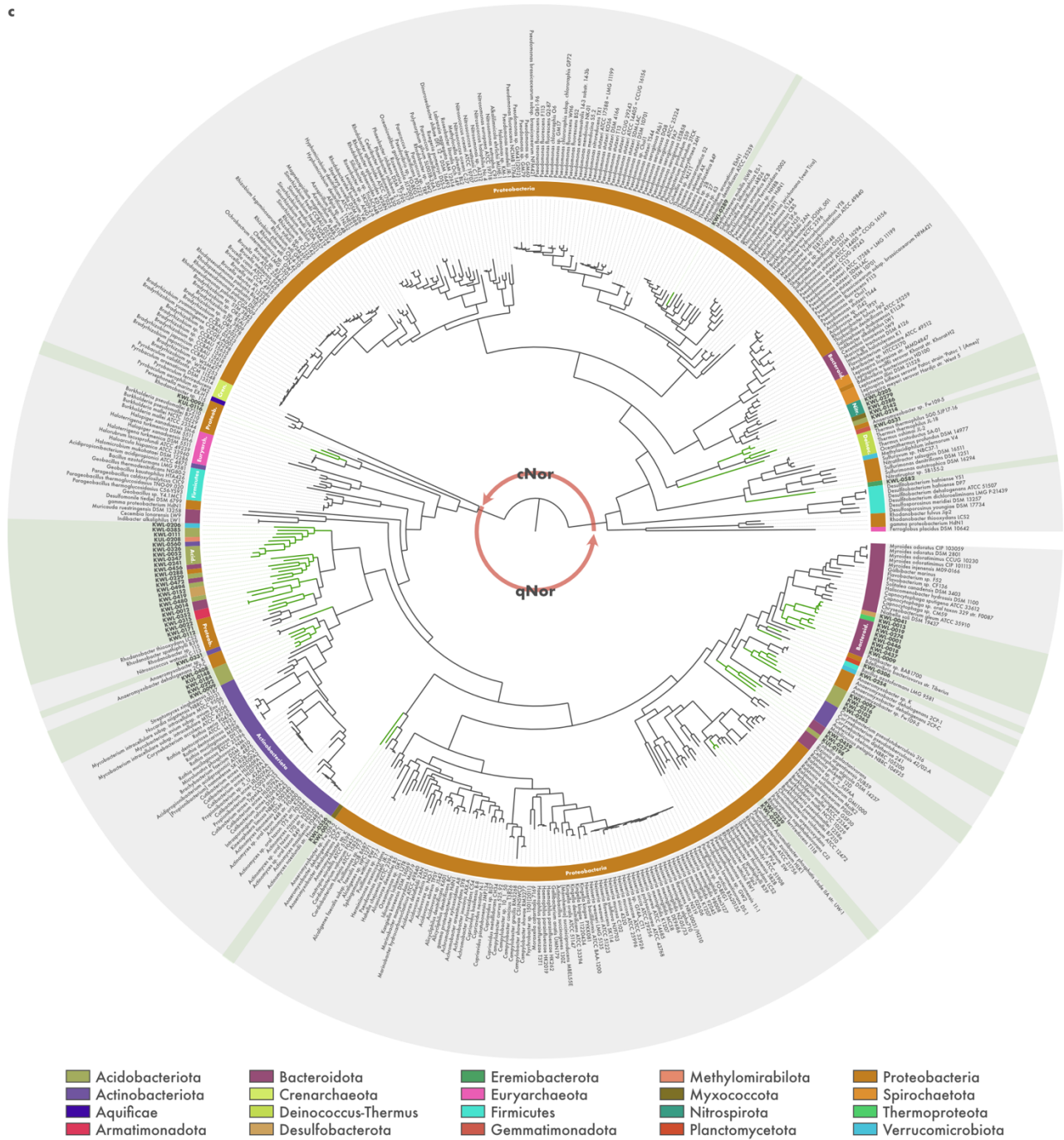
b



907 **Suppl. Fig. S5 (continued) | Phylogeny of a) *nirK*, b) *nirS*, c) *norB*, and d) *nosZ***  
 908 **sequences from metagenome-assembled genomes (MAGs) recovered from tundra**  
 909 **soils in Kilpisjärvi, northern Finland.** Midpoint-rooted maximum-likelihood trees of  
 910 translated sequences from Kilpisjärvi MAGs (highlighted) along with reference sequences from  
 911 archaeal and bacterial genomes.

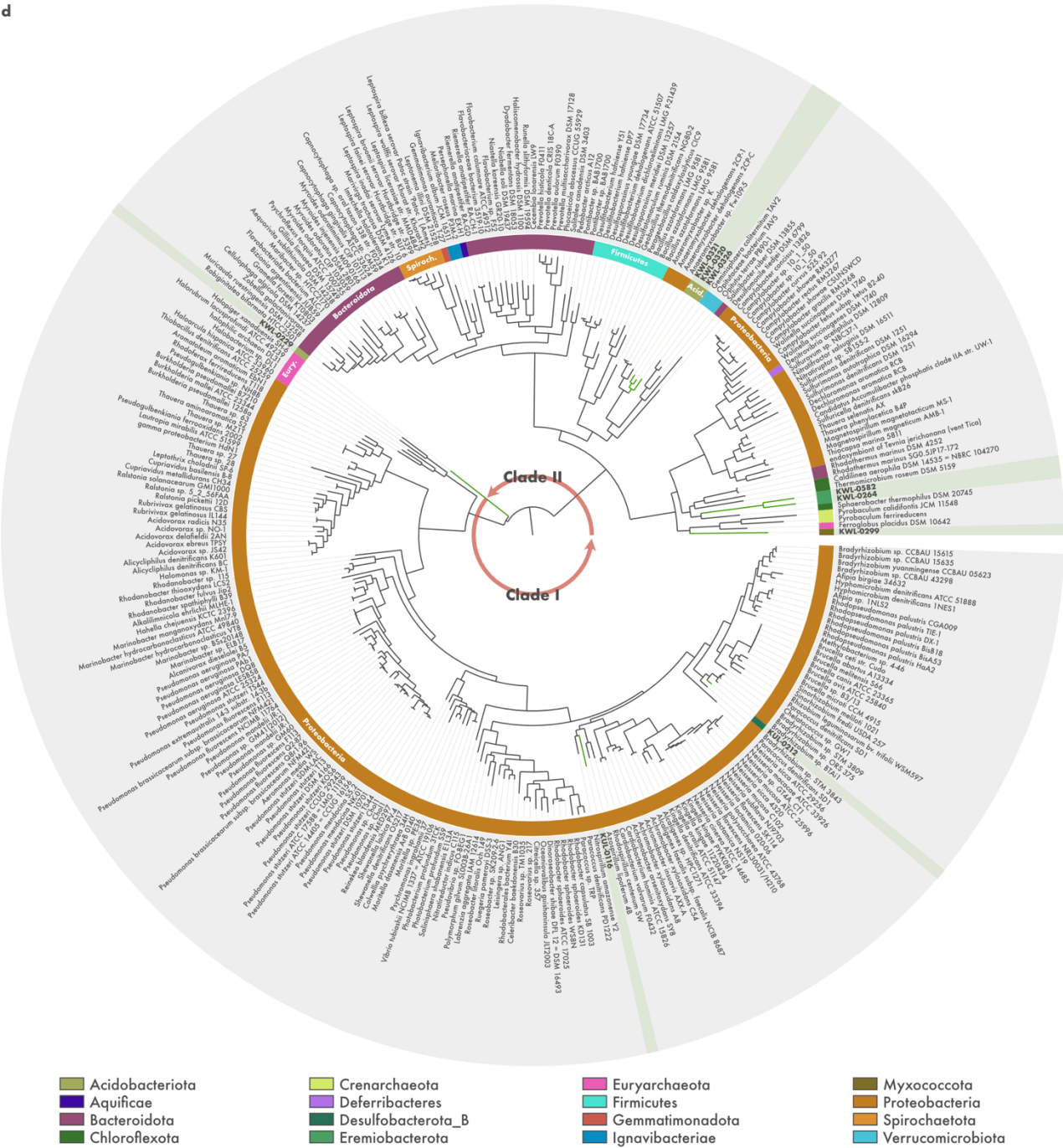


c

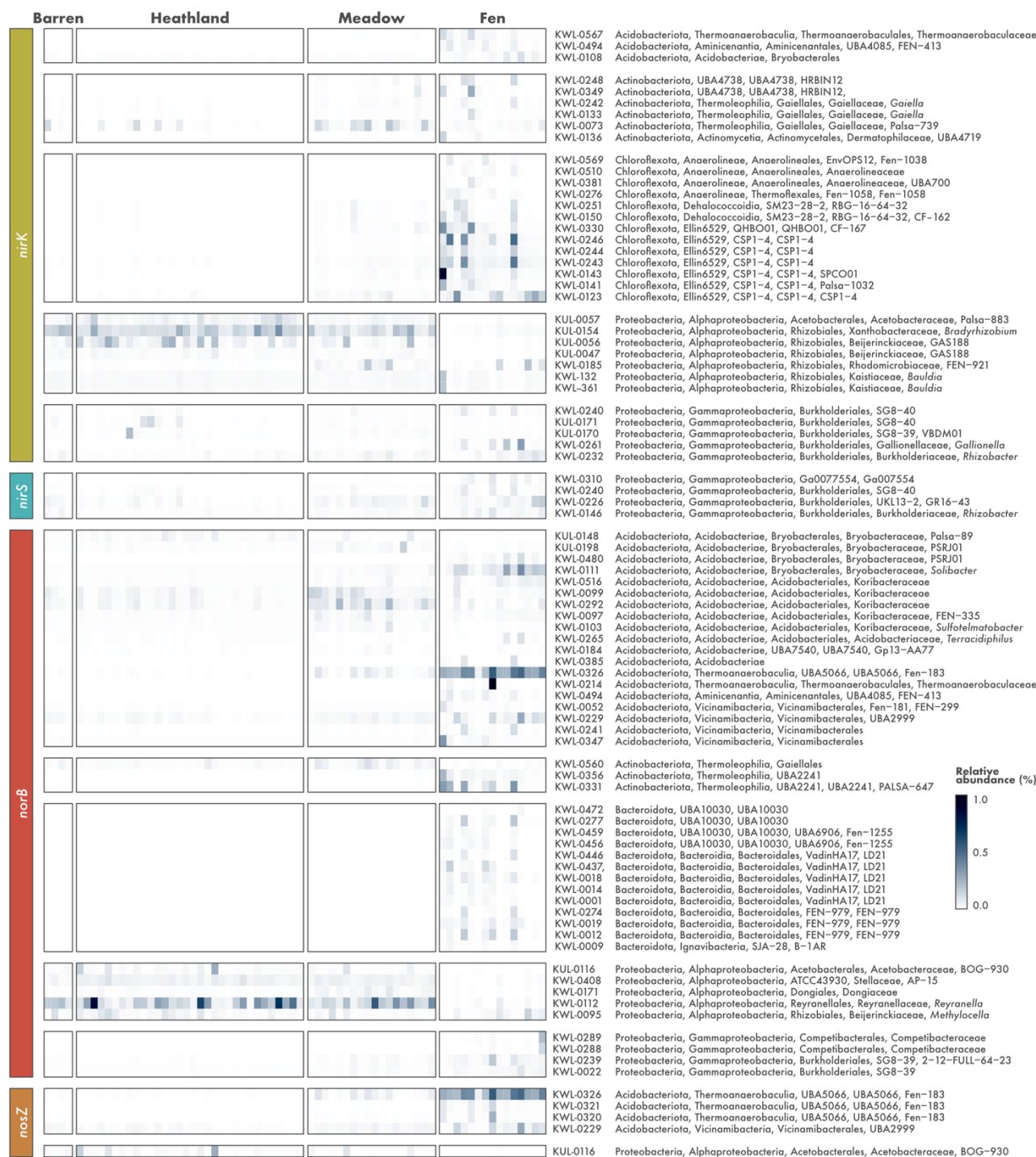


912 **Suppl. Fig. S5 (continued) | Phylogeny of a) *nirK*, b) *nirS*, c) *norB*, and d) *nosZ***  
 913 **sequences from metagenome-assembled genomes (MAGs) recovered from tundra**  
 914 **soils in Kilpisjärvi, northern Finland. Midpoint-rooted maximum-likelihood trees of**  
 915 **translated sequences from Kilpisjärvi MAGs (highlighted) along with reference sequences from**  
 916 **archaeal and bacterial genomes.**

d



917 **Suppl. Fig. S5 (continued) | Phylogeny of a) *nirK*, b) *nirS*, c) *norB*, and d) *nosZ***  
 918 **sequences from metagenome-assembled genomes (MAGs) recovered from tundra**  
 919 **soils in Kilpisjärvi, northern Finland. Midpoint-rooted maximum-likelihood trees of**  
 920 **translated sequences from Kilpisjärvi MAGs (highlighted) along with reference sequences from**  
 921 **archaeal and bacterial genomes.**



922 **Suppl. Fig. S6 | Relative abundance of metagenome-assembled genomes (MAGs)**  
 923 **harbouring denitrification genes across different soil ecosystems in the tundra. MAGs**  
 924 were recovered from soils in Kilpisjärvi, northern Finland, and annotated for genes encoding  
 925 the nitrite (*nirK/nirS*), nitric oxide (*norB*), and nitrous oxide (*nosZ*) reductases using a three-  
 926 step approach. Relative abundances were computed as a proportion of reads mapping to each  
 927 MAG.